



Flood Hazard Assessment for a Hyper-Tidal Estuary as a Function of Tide-Surge-Morphology Interaction

Charlotte Lyddon^{1,2} · Jennifer M. Brown² · Nicoletta Leonardi¹ · Andrew J. Plater¹

Received: 19 July 2017 / Revised: 31 January 2018 / Accepted: 12 February 2018 / Published online: 7 March 2018
© The Author(s) 2018. This article is an open access publication

Abstract

Astronomical high tides and meteorological storm surges present a combined flood hazard to communities and infrastructure. There is a need to incorporate the impact of tide-surge interaction and the spatial and temporal variability of the combined flood hazard in flood risk assessments, especially in hyper-tidal estuaries where the consequences of tide and storm surge concurrence can be catastrophic. Delft3D-FLOW is used to assess up-estuary variability in extreme water levels for a range of historical events of different severity within the Severn Estuary, southwest England as an example. The influence of the following on flood hazard is investigated: (i) event severity, (ii) timing of the peak of a storm surge relative to tidal high water and (iii) the temporal distribution of the storm surge component (here in termed the surge skewness). Results show when modelling a local area event severity is most important control on flood hazard. Tide-surge concurrence increases flood hazard throughout the estuary. Positive surge skewness can result in a greater variability of extreme water levels and residual surge component, the effects of which are magnified up-estuary by estuarine geometry to exacerbate flood hazard. The concepts and methodology shown here can be applied to other estuaries worldwide.

Keywords Flood hazard · Hyper-tidal · Severn estuary · Storm surge · Extreme water level · Delft3D

Introduction

Coastal zones worldwide are subject to the impacts of short-term, local variations in sea-level, particularly communities and industries developed on estuaries (Pye and Blott 2014). Extreme sea levels, caused by the combination of astronomical high tides and meteorological storm surges, are a major threat to coastal communities and infrastructure (Elliott et al. 2014; Quinn et al. 2014; Webster et al. 2014; Prime et al. 2015). This is of particular significance in hyper-tidal estuaries, where tidal range exceeds 6 m (Davies 1964; Robins et al. 2016).

Tidal range can exceed 6 m as tides are amplified through an estuary due to near resonance, shallow bathymetry and

channel convergence (Archer 2013; Pye and Blott 2014). Surges can also be amplified through hyper-tidal estuaries, due to reduced hydraulic drag caused by greater mean depths, as seen along the Orissa coast of India (Sinha et al. 2008) and narrowing topography and orientation of the coastline, as seen in the Cape Fear River Estuary, North Carolina (Familkhalili and Talke 2016). Maximum water levels and storm surge impacts are not simply linearly related to increased tidal range (Spencer et al. 2015), but the complex interactions seen in hyper-tidal estuaries between tide, surge and landscape changes increases sensitivity to timing of storm events (Desplanque and Mossman 2004), and thus exaggerate water levels. Tidal amplification and extreme surge development in hyper-tidal estuaries means concurrence of a large astronomical tide and extreme surge can be catastrophic, as seen in the Bay of Fundy, Canada (Desplanque and Mossman 1999), Meghna Estuary, Bangladesh (As-Salek and Yasuda 2001) and Severn Estuary, UK (Pye and Blott 2010).

Accurate prediction of extreme water level and its timing is essential for storm hazard mitigation in heavily populated and industrialised, hyper-tidal estuaries (Williams and Horsburgh 2013). Such prediction requires accurate understanding of the tide-surge propagation, how this varies as a function of the timing and shape of the storm surge relative to high water

Communicated by Arnaldo Valle-Levinson

✉ Charlotte Lyddon
C.E.Lyddon@liverpool.ac.uk

¹ School of Environmental Sciences, University of Liverpool, L69 7ZT, Liverpool, UK

² National Oceanography Centre Liverpool, Joseph Proudman Building, 6 Brownlow Street, Merseyside L3 5DA, Liverpool, UK

and how such interaction changes due to estuary morphology and bathymetry.

The Bay of Fundy, between the Canadian provinces of New Brunswick and Nova Scotia, has a maximum mean spring tidal range of 16.9 m which is the largest in the world (Greenberg et al. 2012). The tidal range is so large due to near resonance with incoming North Atlantic tides (Desplanque and Mossman 1999) and shallow water depths amplify the tide through the bay (Marvin and Wilson 2016). Shallow water depths and dimensions of the bay also amplify extra-tropical storm surges through the bay (Desplanque and Mossman 2004). Therefore, when a surge coincides with an amplified, high astronomical tide, the results may be little short of catastrophic (Desplanque and Mossman 1999). The concurrence of a rapid drop in pressure and a ‘higher than normal’ tide meant that water levels were elevated 2.5 m above predicted level on the Groundhog Day storm, 1976 (Desplanque and Mossman 2004).

The narrow geometry of the Qiantang River, east China, has a maximum tidal range of 7.72 m at Ganpu at its head and produces one of the world’s largest tidal bores which reaches up to 9 m and travels up to 40 km/h (Pan et al. 2007; Zhang et al. 2012). On the Qiantang River, concurrence of high tide and typhoon-induced storm surges can raise observed water levels up to 10 m above predicted levels (Chen et al. 2014).

Extreme water level events are exaggerated in hyper-tidal estuaries due to the amplified tide-surge propagation, which in turn can increase flood hazard. Flood hazard is defined as the possibility of flood event occurring which could be damaging and harmful to communities and infrastructure (Shanze 2006; Kron 2009). Expansion of the energy and agricultural sector, migration and residential development in the coastal zone can increase flood hazard in estuaries (Pottier et al. 2005; McGranahan et al. 2007). Shanghai, on the Yangtze River Estuary, is a centre for human population and economic activities, with flood hazard further exacerbated by land subsidence (Wang et al. 2012a). Coastal flood hazard analysis aims to understand the processes and dynamics of coastal flooding to assess the potential consequences for people, businesses, the natural and built environment (Narayan et al. 2012; Monbaliu et al. 2014). However, the coastal flood system is a dynamic and complex system, with both physical and human elements possibly exacerbating hazard. Decision-makers must therefore employ a variety of system level analysis models and frameworks that account for key elements of the flooding system to understand the hazard (HR Wallingford 2003).

The commonly used source-pathway-receptor-consequence (SPRC) model identifies key links between the built and natural environment and sources of physical change (Gouldby and Samuels 2005; Horrillo-Caraballo et al. 2013; Oesterwind et al. 2016). This model was adopted by the Environment Agency for local scale, coastal flooding to describe floodwater

propagation from source to floodplains, including physical processes and drivers, infrastructure and strategy (HR Wallingford 2004; Narayan et al. 2012). The first component of the SPRC model are the physical characteristics of flood hazard; sources which may result in flooding events such as intense rainfall and storm astronomical high tides and storm surges. However, quantifying sources in dynamic, interlinked systems can be complex. Spatial and temporal variations in tidal levels, wave setup and rainfall and interaction between sources, natural variability and combinations of sources are hard to account for (Sayers et al. 2002; HR Wallingford 2003). Therefore, there is a need to better understand variability and combinations of physical processes driving local flood systems to improve flood hazard assessment.

Accurate prediction of the combination of factors driving extreme water levels is a key component of understanding and assessing flood hazard (Pender and Néelz 2007). Numerical models can be used to simulate physical processes and calculate rates of change across time and space that result from different combinations of variables, e.g. meteorological conditions, tidal conditions and coastal defence systems (Lewis et al. 2013; Quinn et al. 2014). Analysis of extreme water levels requires a hydrodynamic model, which is able to simulate the flow and velocity of water, for example FVCOM, POLCOMS, TELEMAC and Delft3D (Jones et al. 2007). Two-dimensional, depth-averaged hydrodynamic models have previously been used to successfully simulate the barotropic hydrodynamics in estuaries to help better understand past events, inform decisions concerning flood hazard and the development of energy resources and coastal defence intervention (Xia et al. 2010; Wang et al. 2012b; Cornett et al. 2013; Maskell et al. 2014). These models rely on accurate bathymetry and boundary conditions when modelling coastal and estuarine areas to limit uncertainties in modelled results (Pye and Blott 2014). Modelling studies which focus on the physical drivers of coastal flood hazard can aid decision-makers and clarify connections in the system.

This research focuses on the Severn Estuary as an exemplar of hyper-tidal estuaries worldwide, due to its national significance for nuclear energy infrastructure (Ballinger and Stojanovic 2010), and where complex interactions influence extreme water level and subsequent flood hazard. The Bristol Channel and Severn Estuary, south-west England, is an example of a hyper-tidal estuary prone to relatively frequent meteorologically-induced surges generated by North Atlantic low-pressure systems (Uncles 2010). For the purposes of this paper, the ‘Severn Estuary’ is taken to include the Bristol Channel. These storm surges can be exacerbated by the estuary’s dimensions and characteristics. The tidal range increases from 6.2 m in the outer Bristol Channel to 12.20 m at Avonmouth as a function of geometry (Pye and Blott 2014).

This paper uses the Severn Estuary, south-west England, as an example to describe the assessment of combined flood hazard in the Severn Estuary resulting from astronomical high tides and meteorological storm surges. A sensitivity study is conducted using long-term tide gauge data to force the model boundary of Delft3D-FLOW to investigate variability of extreme water levels. The effect of river flow on extreme water levels is not considered here, because the sensitivity of the Severn Estuary to river flow is not as great as tidal and meteorological drivers. Also the greatest implications of flood hazard upon various nuclear infrastructure will result from tide-surge propagation especially because this is a hyper-tidal estuary. River flow would be an important factor to consider in estuaries with smaller tidal ranges or greater discharge, e.g. Pearl River Delta in China (e.g. Hoitink and Jay 2016; Leonardi et al. 2015). The results show the severity of the combined tide and storm surge event, timing of the peak of the surge relative to tidal high water and the surge skewness are important controls on flood hazard in estuarine environments. This methodology can be applied to other estuaries worldwide, in the context of the SPRC model to help to better understand past extreme events and inform local management needs to minimise future flood hazard.

Methods

Delft3D

Delft3D-FLOW, an open source, hydrodynamic model which solves depth-averaged unsteady shallow-water equations across a boundary fitted grid (Lesser et al. 2004), is used to simulate barotropic tide-surge-river propagation and interaction in the Severn Estuary. The Delft3D-FLOW module has been used in a number of studies to simulate tide-surge propagation and extreme water levels in a coastal environment (Irish and Cañizares 2009; Condon and Veeramony 2012).

Model Domain

The Severn Estuary model domain (Fig. 1) extends from Woolacombe, Devon and the Rhossili, Gower Peninsula in the West, up to Gloucester in the East, which is the tidal limit of the Bristol Channel (Pye and Blott 2010). The 2DH curvilinear grid closely follows the coastline of the Severn Estuary. The horizontal model grid cell size varies from 3 km at the seaward boundary in the lower estuary to less than 10 m in the upper estuary. The model domain has two open boundaries: a sea boundary forced by 15 min tide gauge water level data to the West, and a river boundary forced by 15 min river gauge water level data from Sandhurst to the East.

Gridded bathymetry data at 50 m resolution (SeaZone Solutions Ltd. 2013) were interpolated onto the model grid. Lack of bathymetric data and poor resolution of data in the upper estuary meant that a uniform value had to be applied north of Epney to the river boundary. The value imposed was 2 m, which represented a more realistic channel depth. Sensitivity analysis has been limited to external barotropic tide-surge forcing and river discharge only and no meteorological or wave forcings have been included in the model. Freshwater has not been considered as it has a lower impact on estuarine circulation and water levels. This is shown by the Richardson number, calculated by Reynolds and West (1988), 0.04–0.4 on spring tides, dependent on depth and breadth of the Severn Estuary. This is so impact of tide-surge propagation and external surge timing on extreme water levels up-estuary can be assessed, which is likely to have the greatest impact upon various nuclear energy infrastructure assets within the estuary.

A 0.1 min time step is used to allow for calculations of the shallow water equations to be solved in the fine resolution grid up-estuary. This is validated against the Courant number for the grid. A uniform 0.025 Manning bottom roughness value is applied to the grid.

Tide gauge locations in Fig. 1 indicate where long-term water level records are available, with which to compare and validate the model results.

Boundary Conditions

Long-Term Tide Gauge Data

Long-term tide gauge records from The Mumbles (Fig. 2a) and Ilfracombe (Fig. 2b), located close to the western boundary of the model domain, are used to force the total and tidal water levels in different model setups. The long-term tide gauge records, collected by the UK Tidal Network (https://www.bodc.ac.uk/data/online_delivery/ntslf/), provide hourly sampled tidal records prior to 1992 and quarter hourly sampled tidal records from 1993 to present day. All high water peaks (astronomical tide + storm surge) in the record from Ilfracombe and The Mumbles were identified and isolated. Sea-level values flagged in the tidal record by the British Oceanographic Data Centre (BODC) as improbable, null or interpolated values were discarded, to ensure only accurate observational data are used to force the model boundary.

While joint probability distribution analysis is a common approach to defining event severity (McMillan et al. 2011a; Williams et al. 2016), here we use percentile values applied to long-term monitoring data. This is because many tide-surge water level combinations have the same severity, making it hard to choose a single event. Although return period analysis provides a statistically representative event, we use observed

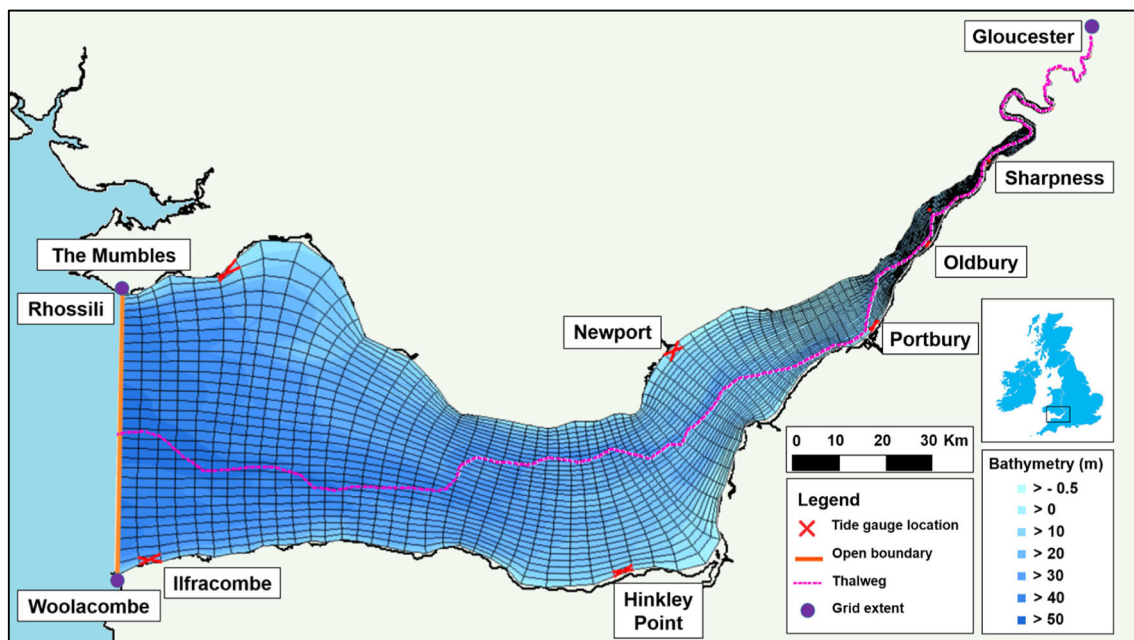


Fig. 1 Severn Estuary model domain. The bathymetry is relative to chart datum (CD)

events and classify their severity against long-term records by the use of percentile values. To identify extreme events at Ilfracombe and The Mumbles, we calculated the 99th, 95th and 90th percentile values of the high water levels and created a set of severity thresholds. Extreme water level events exceeding the 90th, 95th and 99th percentile severity thresholds are identified. Four extreme water level events for which a positive surge occurs and a complete total water level series are available at Ilfracombe or The Mumbles and the tide gauge locations up-estuary (Hinkley, Newport, Portbury, Oldbury, Sharpness, Fig. 1) for validation purposes are identified. Using the Environment Agency return period for still water, extreme sea level values these events fall within the range between a 1/1 (5.41 m) and 1/100 (6.03 m) year event (McMillan et al. 2011b). A historical water level event which falls within the 1/200 year category would be defined as a more severe event. Missing data in the tide gauge records did not allow for data from both Ilfracombe and The Mumbles to be interpolated across the seaward open boundary in the model.

Small differences are present in the tide-gauge records for amplitude and phase between Ilfracombe and The Mumbles. The maximum difference in phase between high water points is 15 min, with high water occurring later at The Mumbles. Small differences occur in amplitude, with a higher water level occurring at the Mumbles, to the order of tens of centimetres. It is likely that tide and surge effects that occur over a region could be coherent at neighbouring stations (Proctor and Flather 1989). The differences could also be an artefact of the recording frequency and could potentially be smaller than observed. Therefore, differences in phase and amplitude are

considered small enough to impose conditions from either location across the sea boundary in a uniform manner.

River level data from Sandhurst river gauge station, located just north of Gloucester, is used to force the eastern model boundary. The river level data is converted to chart datum, to match the model datum.

Surge Characteristics

The extreme water level event is isolated as a storm tide, 6 h before and 6 h after the maximum water level. Water level time series are isolated from the tide gauge record from 3 days prior to and 2 days after the storm tide peak; each model run scenario is 5 days long. Following these criteria, it can be seen that only events since 2012 are taken from the tide gauge record. A notably stormy winter in 2013/2014 coincided with the peak of the 18.6 year tidal lunar cycle (Gratiot et al. 2008; Haigh et al. 2016).

The surge component time series during the 5-day simulations is separated from the total water level time series. Long-term tide gauge records provide information on both total water level and residual surge. The residual surge is calculated as the total observed water level minus the predicted tide, taken from POLTIPS3 which is available from the National Tide and Sea Level Facility (Prime et al. 2015). This way, any tide-surge interaction remains within this residual surge component. A Chebyshev type II, low pass filter is applied to the residual surge component to separate out the time-varying meteorological residual and the tide-surge interactions (an approach used by Brown et al. 2014). The low pass filter is designed to remove all energy at tidal frequencies, using a stop-band of 26 h and a

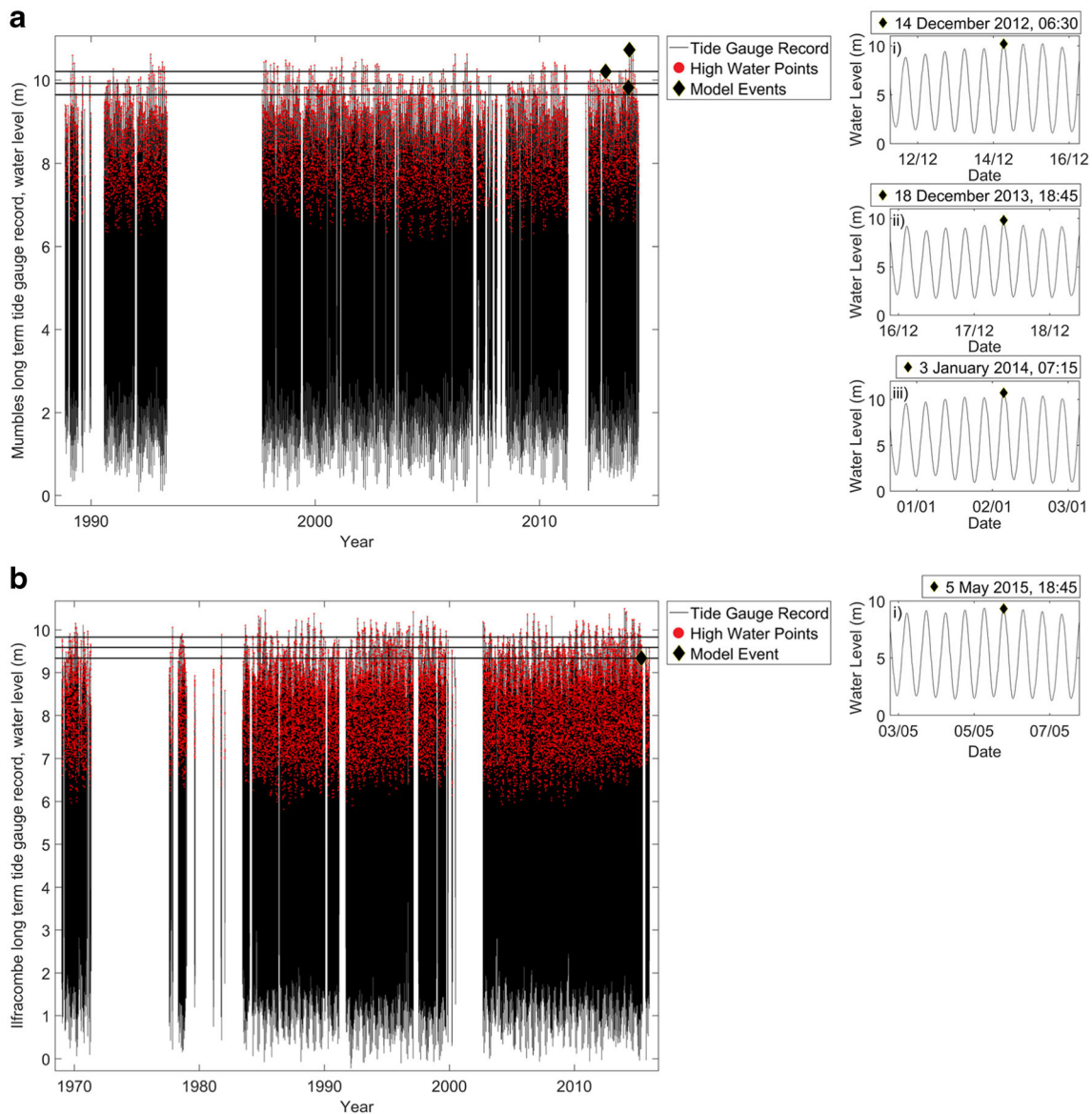


Fig. 2 a Long-term tide gauge record at The Mumbles, Bristol Channel, UK showing tide gauge time series, points in the time series representing high water peaks and events to be modelled. The panels on the right illustrate the three selected events representing the 95th (i, 14th December 2012), 90th (ii, 18 December 2013) and 99th (iii, 3 January

2014) water level percentile values. **b** Long-term tide gauge record at Ilfracombe, Bristol Channel, UK showing tide gauge time series, points in the time series representing high water peaks and events to be modelled. The panel on the right illustrates one selected event representing the 95th (i.e. 5 May 2015) water level percentile values

pass-band of 30 h. A 3 dB pass-band ripple and 30 dB stop-band attenuation was used, to leave only the meteorological residual (low-frequency surge component with no tidal energy or tide-surge interaction) in the time series. Tidal energy and tidal interaction is removed, as it has a similar frequency to the tide and leaves only the low-frequency (> 30 h, sub-tidal) residual (Brown et al. 2014). The low pass filter approach was validated using the 25 h running mean of the surge component.

Storm surge features are characterised by the skewness of the residual surge component with time. Skewness is a measure of the asymmetry of the data around the time series

mean (Gronewald and Meeden 1984). The skewness of a distribution is defined as follows:

$$\text{skewness} = \frac{N}{(N-1)(N-2)} \sum \left[\frac{x_i - \bar{x}}{s} \right]^3$$

where N is the number of observations, x_i is the i th observation, \bar{x} is the mean of the observations and s is the standard deviation of the sample (Gronewald and Meeden 1984). Positive skewness describes a shorter, steeper rising limb on the surge; negative skewness refers to a shorter, steeper falling limb following the maximum surge.

Two events have a surge component with positive skewness, and two with negative skewness. The skewness value of the filtered surge component as defined in this manuscript (asymmetry of the shape of the surge curve) must not be confused with a ‘skew surge’ (the difference between the maximum observed water level and the maximum predicted tidal level, regardless of timing (de Vries et al. 1995)).

To investigate the effects of skewness of the surges on extreme water level, four historical events are presented based on the characteristics of the filtered residual surge component with time (Fig. 3).

Results from the 99th water level percentile event (3 January 2014), the most extreme event on record, shows a high, positive skewness value of 0.59 from the filtered surge data. This indicates that the surge has a longer falling limb; the influence of the surge is extended over time after the peak of the surge. The filtered surge component for the 90th water level percentile event (18 December 2013) shows a lower, positive skewness value of 0.41. This is a lower skewness value than the 99th water level percentile event (3 January 2014), but still indicates a longer falling limb of the surge curve.

The filtered surge component for the 95th water level percentile event (5 May 2015) shows a negative skew value of -0.45 . This indicates a long rising limb of the surge. The filtered surge component for the 95th water level percentile event (14 December 2012) shows a negative skewness value of -0.14 . This value also still indicates that the filtered surge component has a longer rising limb; the influence of the surge is extended over time before the peak of the surge.

Timing of Surge Occurrence

The filtered surge component is recombined with the predicted tide at the tide gauge locations in a range of different time-shifted configurations (McMillan et al. 2011a). The peak of

the surge changes in time relative to the peak of high water to investigate the influence of the timing of the surge on the total water level throughout the estuary.

The first time series represents the realistic timing of the peak of the surge relative to high water for each extreme water level. An additional 13 time series are created with the peak of the surge changing relative to the peak of high water. Starting from a configuration where the peak of the surge coincides with the peak of high water, the peak is then advanced incrementally to 6 h before and delayed equally incrementally to 6 h after high water to cover 1 full tidal cycle.

A total of 16 model runs are thus completed for each historical extreme water level event (Table 1). One validation run is completed for each historical event to ensure the model can reproduce the tide gauge data at stations up-estuary. For this validation model run, the boundary is forced by the total water level time series from Ilfracombe or The Mumbles tide gauge. A ‘tide only’ model run is simulated to provide a baseline, and a number of filtered surge plus tide model runs are simulated to represent the possible timings of the peak of the surge relative to predicted tidal high water.

Model Validation

Water level time series at tide gauge locations in the estuary are isolated from the model outputs. The model is initially validated using the most extreme event on record; with a storm tide peak which occurred at 07:15 on 3 January 2014. The model has been validated at the coast to observation data from tide gauges up-estuary, using data from the UK Tidal Network, Environment Agency and Magnox at Oldbury. Error metrics (R^2 , RMSE, Willmott Index of Agreement (Willmott 1981; Willmott et al. 2012), Bias of the maximum value) are calculated at tide gauge locations up-estuary for model runs with realistic timings of the surge peak relative to tidal high water (total water level, filtered surge + tide) and the

Fig. 3 Normalised filtered surge shape component with time, characterised by historical event severity and skewness (measure of asymmetry)

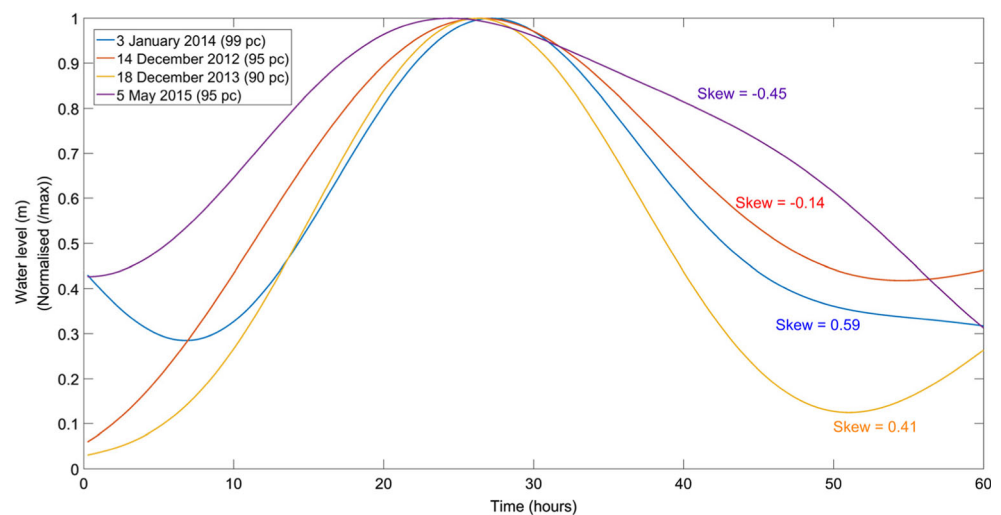


Table 1 Scenarios modelled in Delft3D for each historical extreme water level event

Model run scenario	Purpose
Total water level	Validation
‘Tide only’	Baseline
Tide + surge	Baseline
Tide + filtered surge at 0 min	Sensitivity timing study
Tide + filtered surge at ± 15 min	
Tide + filtered surge at ± 30 min	
Tide + filtered surge at ± 45 min	
Tide + filtered surge at ± 1 h	
Tide + filtered surge at ± 3 h	
Tide + filtered surge at ± 6 h	

tide only simulation to provide a baseline. Error metrics confirm if the model can reproduce observational tide gauge data and assess the error introduced by this methodology.

Figure 4a illustrates validation runs and observational data for Hinkley Point; there is good graphical and statistical agreement between the model output (dashed lines) and observational data (solid line). The model is able to reproduce the tide gauge data at Hinkley Point well, with an R^2 value of 0.996 (Table 2). High water levels are over estimated, as confirmed with a bias value of 0.242, by 15–20 cm. However, this represents just 1.5% of the overall tidal range (12.29 m at Hinkley Point).

The ‘tide only’ model provides a baseline which subsequent model runs can be compared with, as there is no meteorological influence. It can be seen the ‘tide only’ model run is not resolving the high water peaks as there is no meteorological influence, and the low water is underestimated, as shown by the negative bias value. There is a bias away from the tide gauge data in a negative direction—the values are all lower than the observation data. The tidal phase is successfully reproduced. The tide + filtered surge model run, where there is no change in timing of the surge from the real event, also overestimates low water. The tide + filtered surge model run is very similar to total water level simulation, suggesting that external tide-surge interaction, which has been filtered out of the boundary conditions, has a small contribution.

Figure 4b shows how the model has been tested further up-estuary, at Sharpness, using river gauge data from the Environment Agency. The quality of bathymetry and geometry of the long, shallow, narrow channel of the River Severn strongly influence the model results up-estuary. The lower Index of Agreement and R^2 value and higher RMSE and bias (Table 3) for the ‘tide only’ model run indicates that surge has a large contribution to total water level in this location up-estuary. There remains good graphical and statistical agreement between model runs (dashed line) and tide gauge data (solid line). Figure 4b

shows that the model is able to capture tidal asymmetry, which refers to the interaction between tidal wave propagation and shallow water impacts due to changes in width and depth of the channel up-estuary (Uncles 1981; Pye and Blott 2010).

The tidal phase is in good agreement; however, some of the high water points are not achieved, which is likely to be due to error in the low-resolution bathymetry influencing the propagation of the tide in the upper estuary; the bathymetric survey will not match the bathymetry at the time of the event. Errors in bathymetry and flushing can explain the poorer simulation of low water than high water at both locations.

The model is in good agreement without the inclusion of meteorological forcing and waves, confirming that the approach is adequate to capture spatial variations in extreme water levels.

Funnelling Effect vs Frictional Effect

The greatest maximum water elevation along the thalweg of the estuary is 8.12 m at 108 km up-estuary, beyond Portbury, when the peak of the surge occurs 15 min before the peak of high water on 3 January 2014 (99th percentile). It can be seen in Figs. 5 and 6 that the maximum water elevation, along the thalweg of the estuary, during each of the four events consistently occurs close to Portbury. After this point, the maximum water elevation begins to fall again.

The tidal amplitude along estuary is determined by competing processes of tidal damping due to friction, and tidal amplification due to funnelling effect and reflection. From the mouth of the estuary up to Portbury, the funnelling effect dominates to amplify the tidal wave as it propagates up the estuary (Dyer 1995). Mean spring tidal range increases up-estuary towards Portbury due to the funnelling effect of coastal topography, the continuously upward slope of the basin and near-resonance of the estuary to the M2 tidal period (Uncles 1981; Liang et al. 2014). Portbury has the second largest mean spring tidal range in the world, approaching 12.2 m (Uncles 2010). Beyond Portbury, the funnelling effect is counteracted by friction. Friction acts to dampen the propagation of the tidal wave (Proudman 1955a). This balance between the funnelling effect and friction determines where overall maximum water level will occur in the estuary.

The sensitivity of the model domain to an applied friction value and the point where the friction and funnelling effect is balanced is investigated.

A higher friction value (Manning = 0.075) and lower friction value (Manning = 0.013) was applied to the model domain for the 99th water level percentile event (3 January 2014) model runs. The range in maximum water elevations along the deepest channel of the estuary for results of the altered friction values are compared to the original model run (Manning = 0.025).

Fig. 4 **a** Validation down-estuary, Hinkley Point tide gauge. **b** Validation up-estuary, Sharpness river gauge. As above

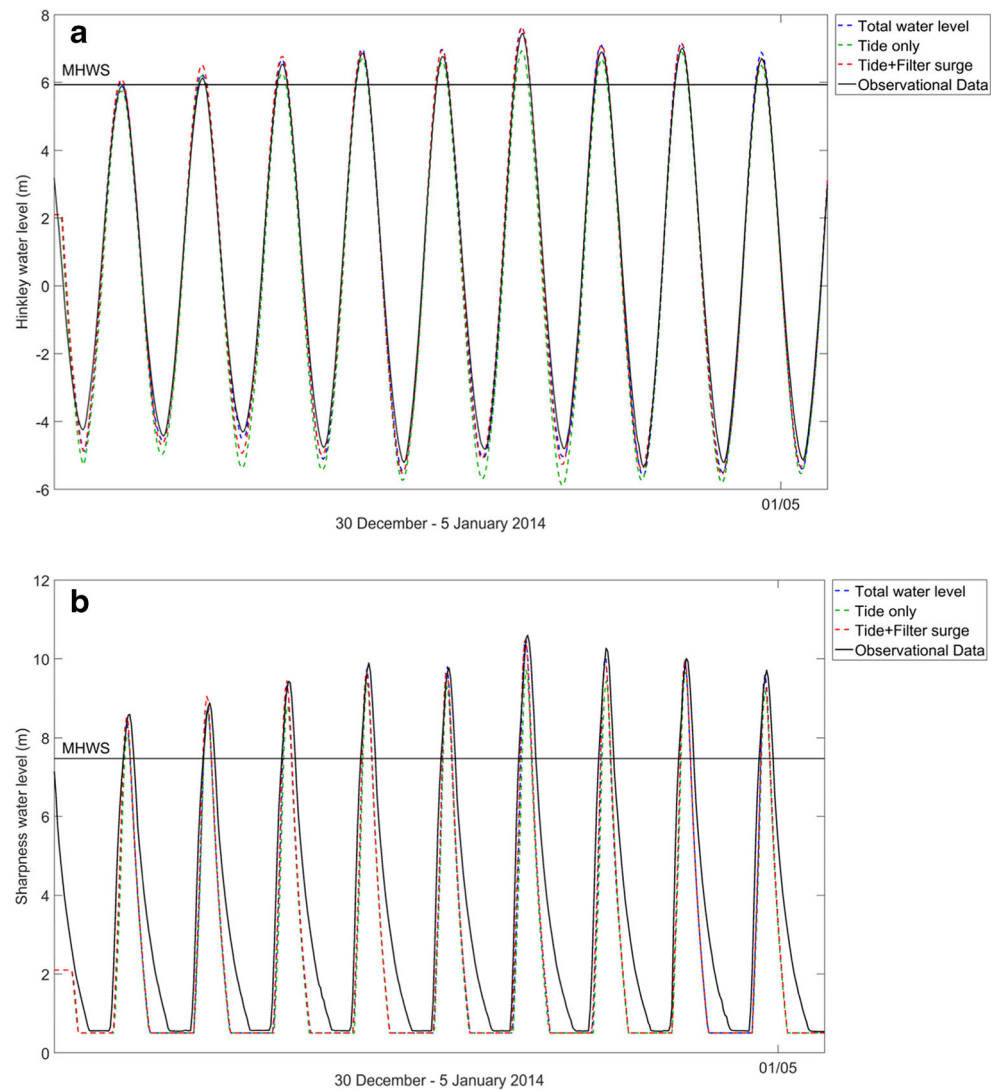


Figure 5 shows that a higher friction value dampens the amplitude of the water elevation from the mouth up-estuary; the funnelling effect has little influence here and there is no obvious tipping point between funnelling and friction. A lower friction value means the funnelling effect significantly amplifies the tidal wave up-estuary, producing water elevations beyond those that would realistically be seen in this estuary. The tipping point between funnelling and friction moves up beyond Oldbury.

The response of the model to changing friction follows the characteristic of tidal response in estuaries (Dyer 1995).

Under a friction value of 0.025, the estuary shows a hypersynchronous response (Fig. 5i) where funnelling effect exceed frictional effects with increasing tidal range up to a point where friction then dominates, due to the shallow, narrow channel morphology. With a low friction value, the estuary responds in a more extreme hypersynchronous manner. Funnelling effects exceed frictional effects throughout the estuary and tidal range continues to increase further up-estuary. Under a high friction value, the model responds in a hyposynchronous manner (Fig. 5 ii). Friction dominates and tidal range diminishes through the

Table 2 Statistical validation down-estuary, Hinkley tide gauge. The filtered surge is applied at a realistic time relative to tidal high water for validation purposes

	Total water level	'Tide only'	Tide + filter surge
R^2	0.996	0.909	0.955
RMS error	0.172	0.255	0.212
Willmott index of agreement	0.969	0.913	0.946
Bias of maximum value	0.242	-0.91	-0.556

Table 3 Statistical validation up-estuary, Sharpness river gauge

	Total water level	‘Tide only’	Tide + filter surge
R^2	0.985	0.897	0.937
RMS error	0.157	0.62	0.206
Wilmott index of agreement	0.9856	0.787	0.97
Bias of maximum value	0.634	-0.609	-0.746

estuary. The funnelling vs friction effect is likely to be a dominating factor in the hydrodynamics of the Severn Estuary, with a change in friction value in the model domain changing where maximum tidal range occurs. Under future sea levels and saltmarsh extents, the estuary dynamics under extreme could change the spatial variability in extreme water levels.

Results

Model outputs are analysed to identify how the total water level, and consequently flood hazard, and local interactions change up-estuary, for different timing of surge occurrence, and surge characteristics. Results are presented systematically for the four extreme events previously selected.

In the first part of the results, variations in maximum water level values along the estuary thalweg, and for different timing of surge occurrence are presented. Changes in water level as a function of surge skewness, and percentile are presented. After that, we will use the following plots as flood hazard proxies at each tide gauge location up-estuary:

- i) Percentage change in maximum total water level compared with the ‘tide only’ model run is plotted as a function of change in timing of surge at the model boundary
- ii) Percentage change in the time integrated elevation, i.e. the area (m^2/s) under the curve of the peak of the storm tide event, exceeding Mean High Water Spring (MHWS) compared with the model run when the peak of the surge and high water coincide (0 min)
- iii) Percentage change in duration (minutes) of the peak of the storm tide event exceeding MHWS, calculated by interpolating between time steps exceeding the MHWS elevation, compared with the ‘tide only’ model run
- iv) Percentage change in maximum total surge elevation, compared with the 0 min model run when the peak of the filtered surge and tide coincide; the total surge is calculated by removing the modelled tidal time series from all total water level model run scenarios, and includes a tide-surge interaction component and a meteorological component. The tide-surge interaction generates harmonics at tidal frequencies, which means that relative contributions cannot be separated

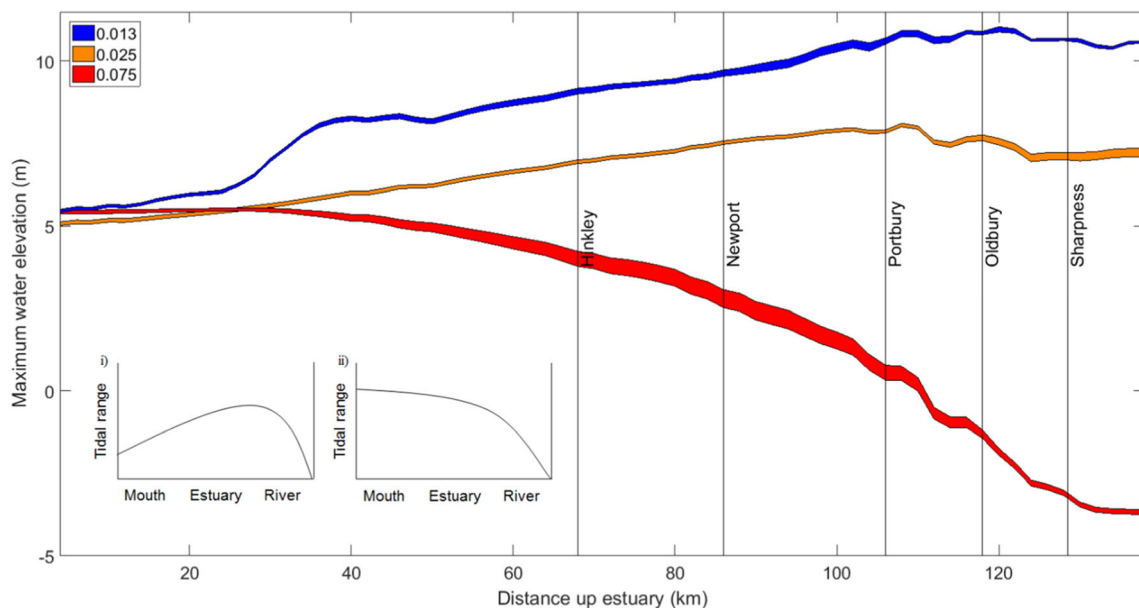


Fig. 5 Water level along the deepest channel in the Severn Estuary, 3 January 2014, under varying Manning friction values (99th percentile); the shading represents the range in results for each filtered surge time shift

scenario. Subpanels show the tidal response of i) hypersynchronous and ii) hyposynchronous estuary to changing frictional effects

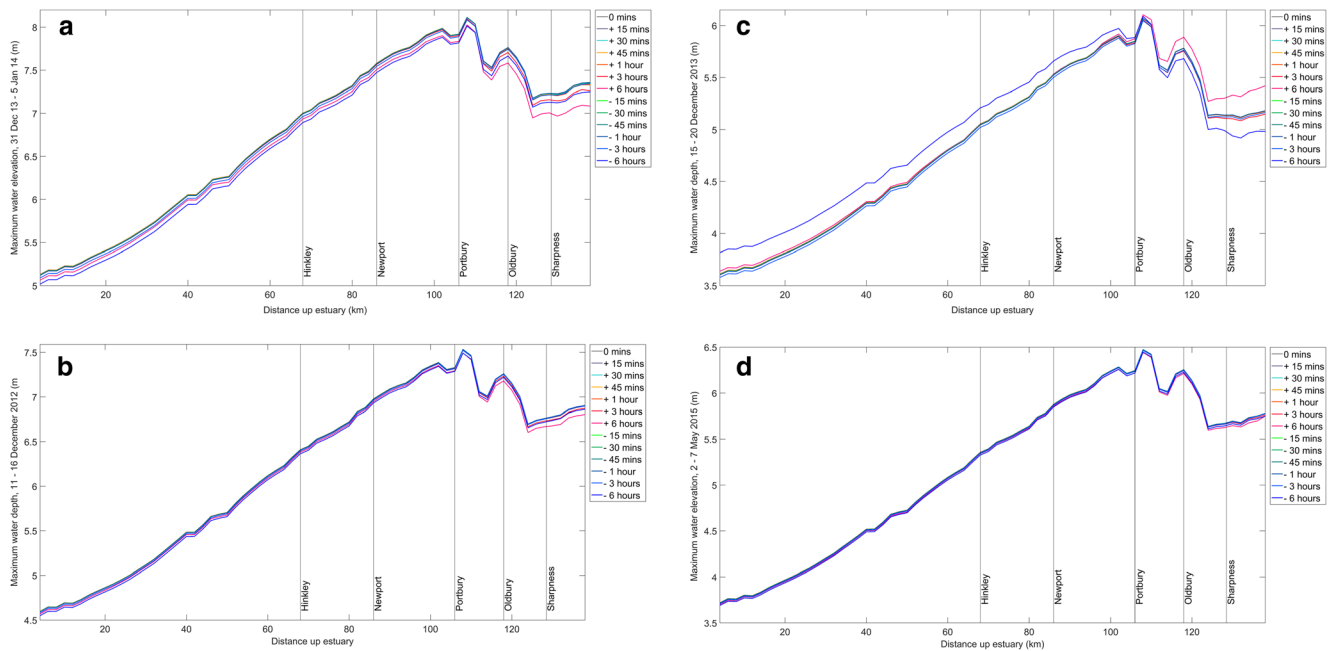


Fig. 6 **a** Maximum water level in the Severn Estuary, 99th water level percentile event (3 January 2014). **b** Maximum water level in the Severn Estuary, 99th water level percentile event (11–16 December 2013). **c** Maximum water level in the Severn Estuary, 95th water level percentile event (14 December 2012). **d** Maximum water level in the Severn Estuary, 95th water level percentile event (5 May 2015)

MHWS is used as the baseline for proxy calculations as this is the reference level for all sea defence designs (McMillan et al. 2011a). All calculated water levels, areas and timings apply to the peak of the storm tide event within the 5-day simulation. The storm tide event is defined as 6 h before and 6 h after the maximum peak of high water in the time series peak. Correlation between each flood hazard proxy, skewness of the filtered surge component and severity of the event is analysed.

Water Level Variations Along Estuary

Figure 6a–d shows maximum water elevation every 2 km along the thalweg of the main channel of the Severn Estuary (Fig. 1) over the duration of the simulation, for each shift in the timing of the peak of the surge relative to tidal high water. The plots illustrate how maximum water elevation changes up-estuary.

It is noticeable from Figs. 6a–d that there is sensitivity to the timing of the peak of the surge relative to tidal high water and there are noticeable changes in maximum water elevations along the deepest channel of the estuary for each time-shifted configuration. Maximum range in water elevations due to surge timing occurred for the 90th and 99th percentile events.

For the 90th water level percentile event (18 December 2013), the highest water elevation down-estuary is seen when the peak of the surge occurs 6 h before the peak of high water. The maximum water elevation down-estuary is consistently 0.2–0.25 m higher than the 0 min scenario when the peak of the surge occurs 6 h before the tidal peak. There is a change in

which scenario results in the highest water elevation at 106.5 km up-estuary. In the upper estuary, the highest water elevation is seen when the peak of the surge occurs 6 h after the peak of high water. The water elevation is consistently 0.1–0.35 m higher than the 0 min scenario, when the peak of the surge occurs 6 h after the tidal peak.

For the 99th water level percentile event (3 January 2014), the highest water elevation down-estuary is seen when the peak of the surge occurs 1 h after the peak of high water. The maximum water elevation down-estuary is consistently 0.2–0.25 m higher than the 0 min scenario when the peak of the surge 1 h after the tidal peak. The minimum water elevation down-estuary is 0.1–0.15 m lower than the 0 min scenario when the peak of the surge occurs 6 h before high water. In the upper portion of the estuary, the highest water elevation consistently occurs 0.01–0.05 m higher than the 0 min scenario when the peak of the surge is 30, 45 or 60 min after high water: there is no scenario which consistently results in the maximum water elevation. However, the lowest water elevation in the upper portion of the estuary is consistently a result of when the surge peak is 6 h before the tidal peak, and is up to 0.25 m lower than the 0 min scenario.

It is noticeable in Fig. 6a–d that change in time of the peak of the surge relative to high water causes little variability in the maximum water elevation in the lower estuary, and greatest variability in water elevation between time shift scenarios beyond Portbury, 106 km up-estuary.

Figure 7 shows the range of maximum water elevation every 2 km along the thalweg for all time shift configurations. The range of values are coloured according to the skewness of

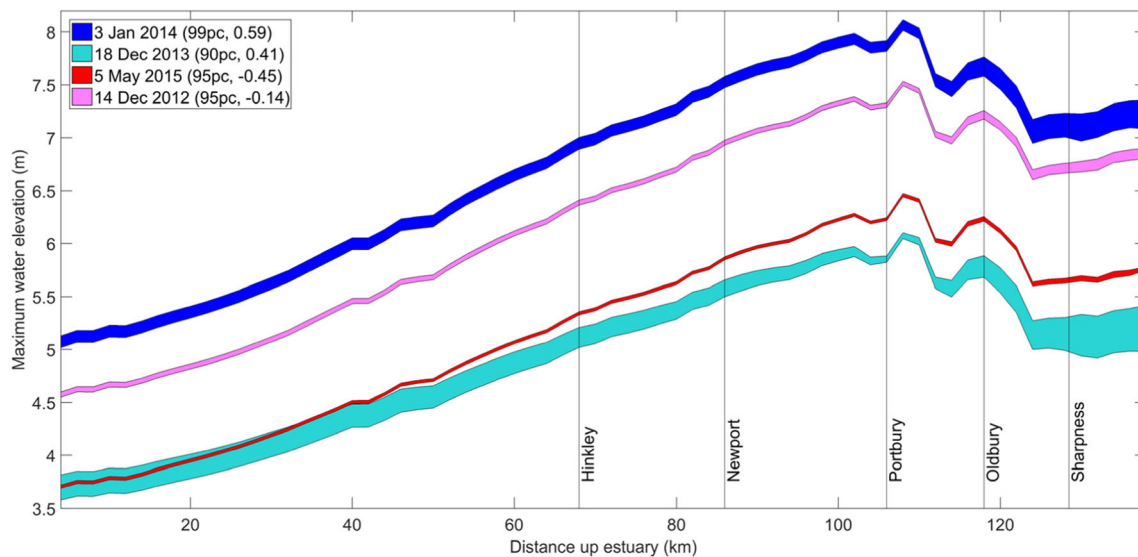


Fig. 7 Range of water level values for time shift configurations along deepest channel of the Severn Estuary when overall maximum water level occurs. For each event, in the legend, the first value represents the percentile of the event and the second value is the skewness

the surge component with time, and also classified based on the severity of the extreme event.

The greatest range between maximum and minimum water elevation across the surge time shift scenarios is 0.44 m for the 90th water level percentile event (18 December 2013) and 0.27 m for the 99th water level percentile event (3 January 2014). Deviations in water level are not uniform along the estuary, and the 90th water level percentile event shows a positive shift in water level in the lower part, and negative shift in the upper part. The surge component of both these events has a positive skewness value. The smallest range between maximum and minimum water elevation across the surge time shift scenarios is 0.03 m, for 95th water level percentile event (14 December 2012). This event has a surge component with a negative skewness value.

The surge components which have a positive skewness value, a steeper rising limb and a longer falling limb show the greatest range of water elevation values along the deepest channel of the estuary. The range of values increases up-estuary, with the greatest range in water level values occurring beyond Portbury. This indicates that location in the upper estuary may be more sensitive to changes in the timing of the peak of a surge which displays a positive skewness. The surge components which have a negative skewness, a longer rising limb and steeper falling limb show a more constrained range of maximum water elevations and there is less sensitivity throughout the estuary to the timing of the surge peak.

The maximum water elevations are stacked on top of each other according to severity of the event. It can be seen that the 99th water level percentile event (3 January 2014) consistently results in the greatest maximum water elevations along the

thalweg of the estuary. The 95th percentile events show less extreme maximum water elevations in the estuary. There is approximately a 1 m difference between the 95th water level percentile event (14 December 2012) and 95th water level percentile event (5 May 2015). The 95th water level percentile event (5 May 2015) initially shows similar water level values to the 90th water level percentile event (18 December 2013), before increasing beyond this 90th percentile event. As expected, the 90th water level percentile event (18 December 2013) shows the lowest maximum water elevations along the deepest channel of the estuary.

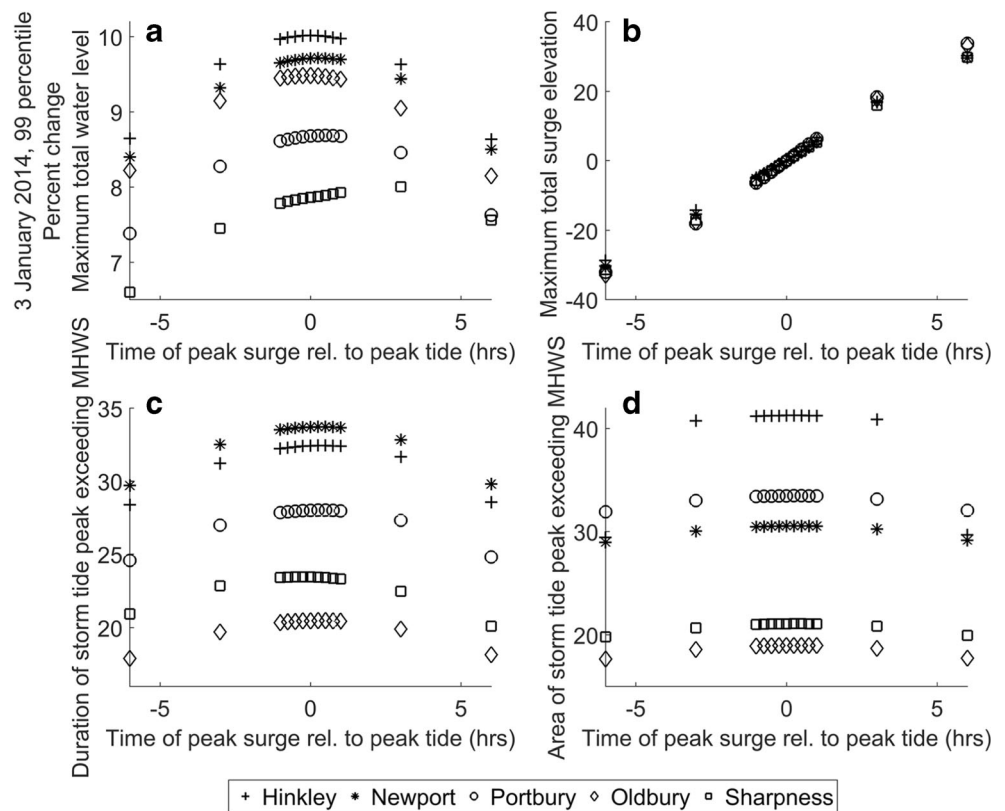
It is also evident in Figs. 6 and 7 that the maximum water elevation for all extreme water level events consistently occurs close to Portbury, the location for maximum observed tidal range in the estuary (Pye and Blott 2014).

Changes in Flood Hazard Proxy with Surge Timing

Figures 8, 9, 10 and 11 show changes in flood hazard up-estuary in locations where nuclear assets and/or tide gauges are located, as a function of change in timing of the surge at the model boundary. Each flood hazard proxy (maximum total water level, maximum total surge, time integrated elevation and duration exceeding MHWs) is calculated from the storm tide peak: 6 h before and 6 h after high water. All data are displayed as percentage change, compared with the ‘tide only’ model scenario, apart from maximum total surge which is compared with the model run when the peak of the surge and high tidal water coincide (‘0 min’).

Figure 8 shows flood hazard at each tide gauge location for a 99th water level percentile event (3 January 2014), the most extreme event on record.

Fig. 8 3 January 2014. Flood hazard proxy calculated at each tide gauge location. **a** Percent change in maximum water level. **b** Percent change in maximum total surge elevation. **c** Percent change in duration exceeding MHWS. **d** Percent change in area exceeding MHWS. All data is displayed as percentage change, compared with the tide only model scenario, apart from non-linear interaction which is compared with the model run when the peak of the surge and high water coincide



The greatest percentage change in maximum total water level between each time shift scenario and the ‘tide only’ scenario is seen in tide gauge locations down-estuary, notably Hinkley Point and Newport (up to 10.02%). Tide gauge locations down-estuary, Hinkley Point, Portbury and Oldbury show symmetry in the results: the highest maximum water level happens when the surge occurs at the same time as high water. The magnitude of the maximum total water level then reduces when the peak of the surge occurs before or after the peak of high tide.

There is less percentage change in maximum total water level at tide gauge locations further up-estuary. The greatest percentage change in maximum total water level occurs when the peak of the surge happens 3 h after the peak of high water. This is particularly clear at Sharpness, up to 8%.

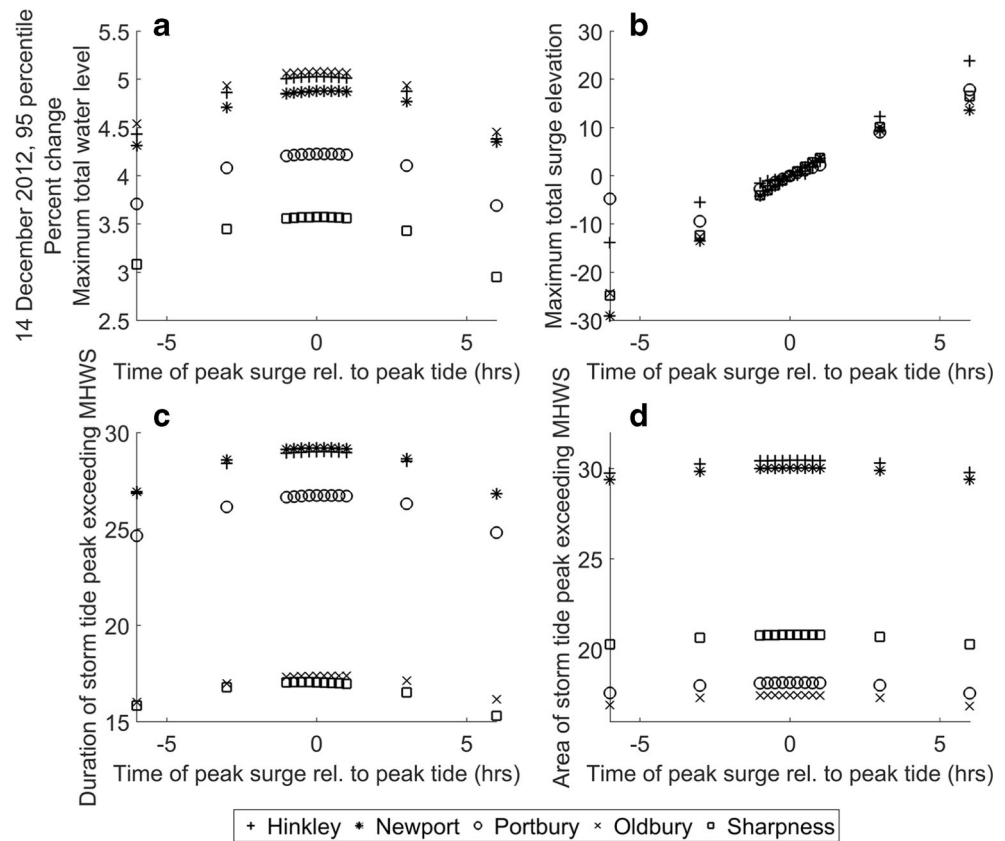
There is a noticeable linear trend in the percentage change of maximum total surge value which occurs ± 6 h of the storm tide peak, compared with the 0 min scenario. The greatest positive percentage change in maximum total surge elevation can be seen when peak of the surge occurs after 6 h after the peak of tidal high water. A similar magnitude of negative percentage change in maximum total surge can be seen when the peak of the surge occurs 6 h before the peak of tidal high water. There is little sensitivity of maximum total surge elevation to the timing of the surge when the peak occurs around the time of high water, and there is also little spatial variability

between the locations. There is increased variability in maximum total surge elevation across the estuary with greater shift away tidal high water. The greatest variability can be seen when the peak of the surge occurs significantly after tidal high water. Portbury shows the greatest positive percentage change in maximum total surge elevation (32.5%) when the peak of the surge occurs 6 h after tidal high water. This could be linked to the positive skewness of the surge with greater influence after the peak.

The maximum change in duration of peak of the storm tide exceeding MHWS is seen at locations down-estuary, Hinkley Point and Newport. Portbury and Oldbury show the greatest change in duration when the peak of the surge occurs 1–3 h after the peak of high water. There is a smaller percentage change in duration of the storm tide peak exceeding MHWS further up-estuary, at Sharpness. These tide gauge locations show asymmetrical results, with the greatest change in duration when the peak of the surge occurs 3 h before the peak of high water.

The greatest change in time-integrated elevation of the peak of the storm tide exceeding MHWS is seen at Hinkley Point, with the greatest area exceeding MHWS when the peak of the surge occurs at the same time relative to the peak of high water. Model results from Portbury and Newport also show over 28% change in time-integrated elevation (m^2) exceeding MHWS. Locations further up-

Fig. 9 14 December 2012. Flood hazard proxy, as in Fig. 8



estuary, Oldbury and Sharpness, consistently show lower percentage change within the range of 17–21%. These results are also symmetrical, with the greatest percentage of change in area when the peak of the surge occurs at the same time as the peak of high water.

Figure 9 shows flood hazard at each tide gauge location for a 95th water level percentile event (14 December 2012). The greatest percentage change in maximum total water level between each time shift scenario and the ‘tide only’ model run is seen in tide gauge locations down-estuary, at Hinkley Point and Newport, up to 5%. Oldbury is located further up-estuary, where the channel of the River Severn begins to narrow, but still shows a greater percentage change than Portbury. The change in maximum water level for this event is not to the same extent as the 99th water level percentile event (3 January 2014). Sharpness shows the smallest percentage change in maximum total water level, compared with the ‘tide only’ model run. All results show a symmetrical shape, with the greatest change in total maximum water level when the peak of the surge coincides with the peak of high water. The smallest percentage change in maximum water level occurs at all locations up-estuary when the peak of the surge occurs 6 h after the peak of high water.

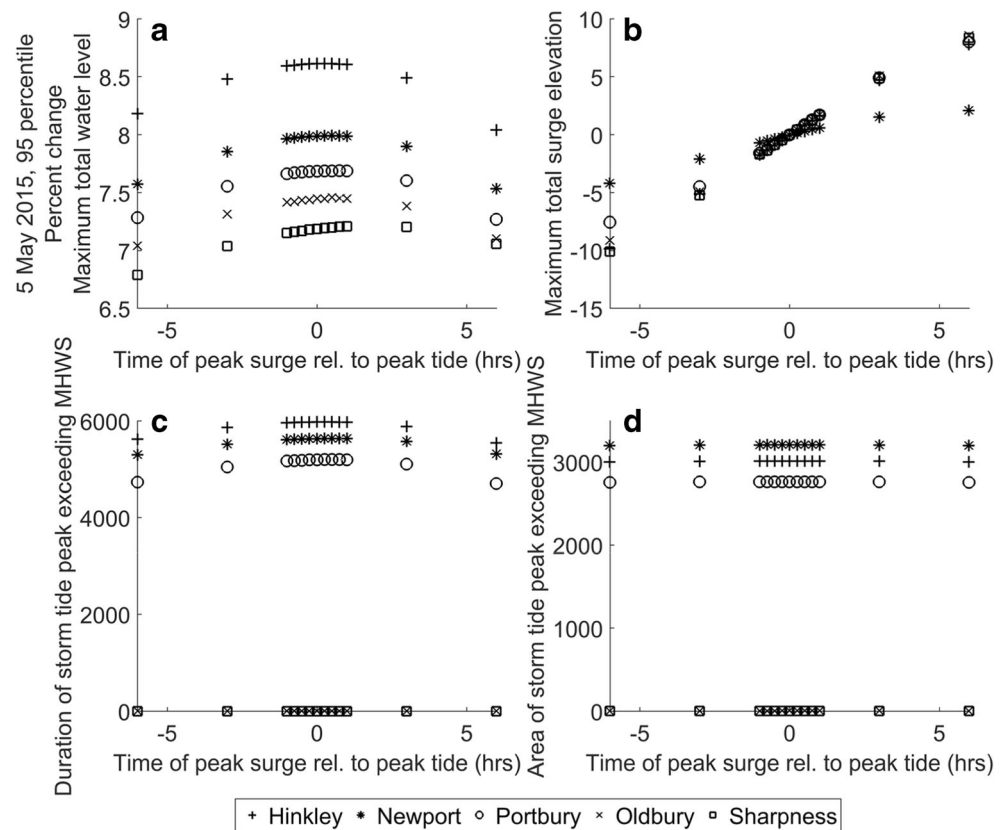
The linear trend in percentage change of maximum total surge elevation for a 95th water level percentile event (14 December 2012) is similar to 99th water level percentile event

(3 January 2014), with the changing time of the peak of the surge relative to tidal high water. The greatest positive percentage change occurs when the peak of the surge occurs significantly after tidal high water, at Hinkley Point (21.2%) and Portbury (17.8%). The greatest variability and magnitude in percentage change of maximum total surge elevation occurs when the surge occurs 6 h before the peak of tidal high water. This could be linked to the negative surge skewness, with greater influence before the peak of the surge. There is less variability in maximum total surge elevation when the surge occurs 6 h after tidal water.

The greatest percentage change in duration of the peak of high water exceeding MHWS is in locations down-estuary, notably Hinkley Point and Newport, up to 29.2%. These locations also show a symmetrical trend; the greatest percentage change is when the peak of the surge occurs at the same time as the peak of high water. The locations are stacked on top of each other, which is determined by the location up-estuary. There is a notable gap in percentage change in duration between locations in the lower estuary (Hinkley Point, Newport) and the upper estuary (Sharpness, Oldbury). Greatest duration at Oldbury and Sharpness is when surge occurs 1 h before high water.

The greatest percentage change in area of the peak of high water exceeding MHWS is in locations down-estuary, notably Hinkley and Newport, up to 30.5%. Locations are stacked on

Fig. 10 5 May 2015. Flood hazard proxy, as in Fig. 8



top of each other, as a function of the distance up-estuary. All locations show symmetrical trends as the peak of the surge changes relative to high water; the greatest change in area is when the peak of the surge and tide coincide. In addition to this, there is less variation between each time shift, and results at each location appear flatter than changes seen in maximum total water level and duration of peak exceeding MHWS.

Figure 10 shows flood hazard at each tide gauge location for a 95th water level percentile event (5 May 2015). The greatest percentage change in maximum total water level, compared with the ‘tide only’ model run, is seen at Hinkley Point, Newport and Portbury, up to 8.6%. As seen in other figures, the locations are stacked on top of each other based on their distance up-estuary. Epney, for example, shows smallest percentage change. All locations show least percentage change at -6 h.

The linear trend in percentage change of maximum total surge elevation is also noticeable for 5 May 2015. There is a smaller overall magnitude of positive and negative percentage change compared to the other events. Sharpness shows greatest negative percentage change (-10%) and Oldbury shows greatest positive percentage change in maximum total surge elevation (8.6%). Newport shows little sensitivity to the changing time of the peak of the surge relative to high water. There is less variability between locations, excluding Newport, when the peak of the surge occurs significantly before or after tidal high water.

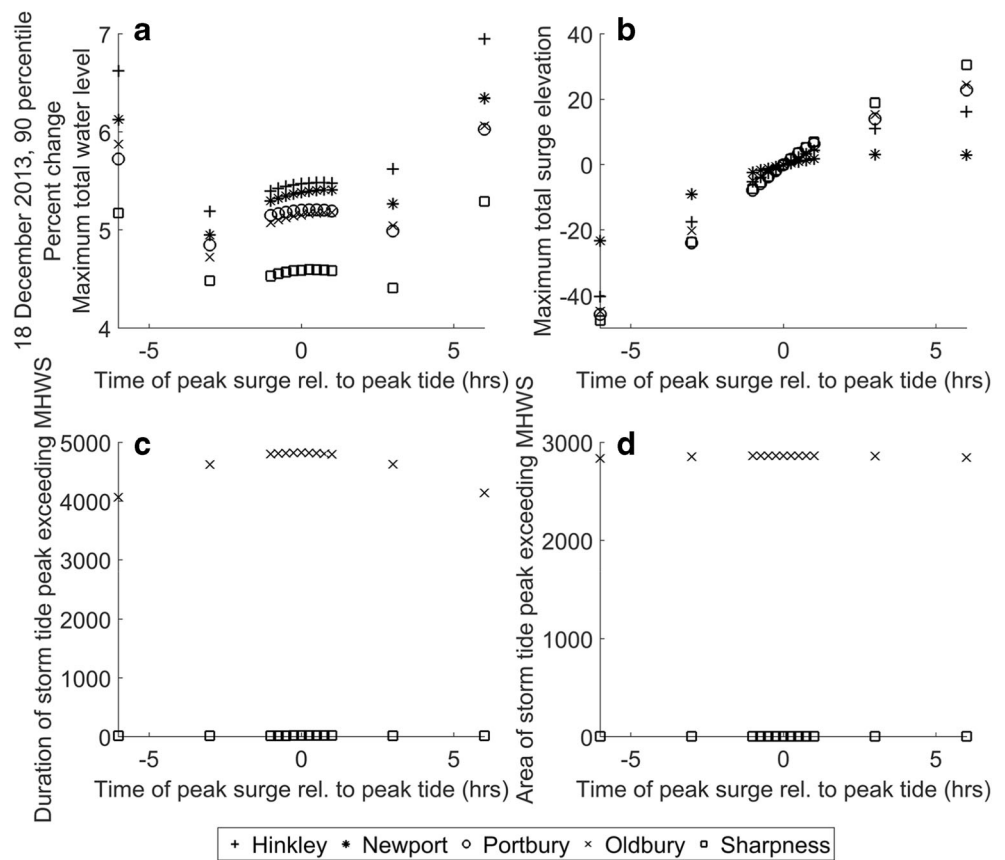
The storm tide peak exceeds MHWS at all locations for a 95th water level percentile event (5 May 2015). Hinkley Point shows the greatest percentage change in duration of the storm tide peak exceeding MHWS, but there are small changes between each time shift scenario.

The greatest change in duration at Portbury occurs at -15 min (11.725%), followed by 0 min (11.72%) and -30 min (11.71%). Small percentage changes occur across all locations (within 0.1% change in duration) when the surge occurs within 1 h of high water. The lowest percentage change at all locations occurs when the peak of the surge occurs 6 h after the peak of high water. This could be due to the influence of the characteristics of the filtered surge that has been modelled for this historical event.

Figure 11a shows flood hazard at each tide gauge location for 90th water level percentile event (18 December 2013). Down-estuary locations, at Hinkley Point, Newport, Portbury and Oldbury, show a similar percentage change in maximum total water level, up to 7% , compared with the ‘tide only’ model run. The smallest percentage change is seen at Sharpness. All locations show a jump in maximum water level at $+6$ and -6 h, which could be due to the influence of the shape of the surge, as the other time shifts show a flatter trend.

The linear trend in percentage change of maximum total surge elevation in Fig. 11a (ii) is similar to other events. There is greater variability between locations when the peak of the surge occurs 3 or 6 h before and after tidal high water like the

Fig. 11 18 December 2013. Flood hazard proxy as in Fig. 8



99th water level percentile event (3 January 2014). This could be linked to surge skewness like the 3 January 2014. The greatest magnitude of percentage change can be seen when the peak of the surge occurs significantly before tidal high water. The greatest positive (29.08%) and negative (−47.57%) percentage change in maximum total surge elevation occurs at Sharpness. Newport shows less sensitivity to the timing of the peak of the surge relative to high water, with a range of 20.1% and a more symmetrical trend.

The peak of the storm tide only exceeds MHWS at Sharpness and Oldbury when the 18 December 2013 event is simulated, likely to be because it is a 90th percentile event. Oldbury shows a clear percentage change because the ‘tide only’ scenario (6.821 m), which all time shift scenarios are compared with, does not exceed MHWS (7.02 m). The surge is having a noticeable influence on the time the peak of the storm tide exceeds MHWS at these locations. Figure 12 shows that Sharpness has an asymmetrical trend with the greatest percentage change in duration (19.9%) when the surge occurs 45 min after high tide.

Oldbury also shows a noticeable percentage change for area exceeding MHWS compared with the ‘tide only’ model run, and a very small value for Sharpness (Fig. 12). Sharpness shows a small range of 0.1% between time-shift scenarios. The greatest change in area (3.9%) happens when the surge occurs 1 h after high tide.

Discussion

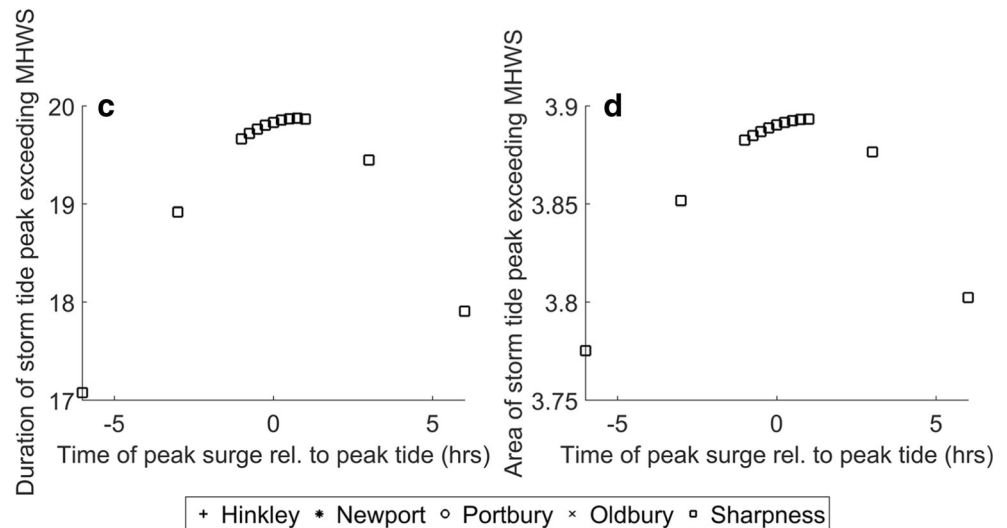
Physical Drivers and Sources of Flood Hazard in the Severn Estuary Model Domain

Delft3D-FLOW is used to simulate barotropic tide-surge propagation, river flow and interaction in the Severn Estuary across a 2DH grid. Results from four historical events are presented which show the influence of the severity of the storm surge, the influence of the timing of the surge on the total water level and characteristics of the filtered surge component on the total water level throughout the Severn estuary. The results presented here can help to identify variability in the sources of an extreme water level event in a hyper-tidal estuary, which can contribute towards flood hazard. These results can help to inform local management needs in a hyper-tidal estuary when viewed in the context of the source-pathway-receptor-consequence (SPRC) conceptual model (Shanze 2006).

Influence of Storm Severity on Extreme Water Levels

The results suggest that severity of the event is an important control on the magnitude of extreme water levels throughout the Severn Estuary. The 99th water level percentile event (3 January 2014) consistently produced greatest water elevations

Fig. 12 Duration and area of storm tide peak exceeding MHWS at Sharpness



along the deepest channel of the estuary and greatest percentage change in maximum water levels at all sites. A more severe storm surge event, driven by low atmospheric pressure, wind speed, wind direction and storm duration (Woth et al. 2006), increases extreme water levels throughout in the Severn Estuary and is an important driver of flood hazard. Extreme tidal levels are known to be the predominant driver of flooding events in the Severn Estuary, particularly in locations close to the maximum MHWS at Avonmouth (Capita Symonds 2011). A 3.54 m (11.6 ft) surge was recorded at Avonmouth in March 1947 (Heaps 1983), attributed to very low pressure (974 mb, which is 38 mb below normal regional level) and predominantly easterly track of the depression (Lennon 1963), indicating the severity of a storm surge event is a combination of meteorological factors.

The 99th percentile water level events may be a rare occurrence, and equal consideration should be given to the effect of more frequent, less severe events in the estuary. However, much of the UK is defended against high-frequency, low-magnitude events up to a 1:200 year event, therefore reducing flood hazard. An understanding that a more severe, extreme water level event can increase flood hazard can be used by local coastal planners to manage flood risk and can aid operational flood management (Menéndez and Woodworth 2010). If the severity of an event can be forecast then warnings can be issued to appropriate authorities and the public (FLOODsite 2005). Event severity is an important control when modelling to extreme water levels on a local scale.

Influence of the Timing of the Peak of the Surge

The timing of the peak of the storm surge relative to tidal high water is another important contribution to the physical drivers of flood hazard at the coast. There is sensitivity to the timing of the peak of the surge throughout the Severn

Estuary model domain. This is particularly evident in the upper estuary; when the peak of the surge occurs 2–6 h after high water, there is a greater percentage change in maximum water level. Increased water depth at the time of tidal high water could induce surge propagation through the estuary (Wolf 2009) to increase extreme water levels up-estuary. Increased water depths would limit shallow water and quadratic friction effects on the tidal amplitude. However, at these shifts, the flood hazard (area and duration of the storm tide peak exceeding MHWS) is lower.

There is less sensitivity to changes in the timing of the surge in the lower estuary, notably Hinkley Point. The greatest percentage change in maximum water level occurs when the peak of the storm surge and tide coincide. The concurrence of high tide and storm surge peak in the Severn Estuary has resulted in extreme water levels in the past (Lennon 1963). The highest recorded water level in the Severn Estuary in a century occurred during the storm 13 December 1981 (Proctor and Flather 1989). A fast moving secondary depression, tracking further south than usual for the time of year, produced strong west to northwesterly gales over the Bristol Channel (Williams et al. 2012). This depression generated a surge peak of 1.5–2 m, which occurred close to the time of high water of a large spring tide (Heaps 1983; Smith et al. 2012). Little warning was given, and the event resulted in severe flooding and damage to property and agricultural land from east of Bideford to Gloucester (Uncles 2010). The timing of the passage of the depression, which was coincident with tidal high water in the Bristol Channel, was a vital contributor to the water levels produced (Proctor and Flather 1989). This event was significant as it highlighted the importance of high-resolution temporal monitoring data during fast moving depressions, and reanalysis atmospheric data for the event has been used to test the accuracy of operational forecasting systems (Williams et al. 2012). A larger storm surge (2.4 m) in the

Severn Estuary on 24 December 1977 occurred 3 h before high water, giving no cause for concern (Proctor and Flather 1989). Surges larger than 2 m rarely occur within 1 h of tidal high water in the Severn Estuary due to locally generated tide-surge interaction (Horsburgh and Horritt 2006). However, there is no mechanism to stop the peak of a spring tide and storm surge coinciding in the Severn Estuary (Pye 2010).

Flood hazard is also increased in the Bay of Fundy when adverse weather conditions, e.g. a drop in pressure greater than 5 kPa, coincides within 1 to 2 h of high water of large spring tides (Greenberg et al. 2012). Significant low-pressure systems have coincided with a very high spring tide on only a few occasions; November 1759, October 1869, during the Saxby Gale and the 1976 Groundhog Day storm (Desplanque and Mossman 2004). During all events, seawalls and wharfs were breached, leading to severe flooding, damage to boats and infrastructure, and lives lost (Desplanque and Mossman 1999). Storms not occurring near high water or on average tides will produce water levels within the ‘normal’ range that are often reached by astronomical tides alone (Desplanque and Mossman 1999). The concurrence of the peak of a storm surge with the peak of spring tidal high water could be rare occurrence, but would cause the greatest impacts on maximum extreme water levels. The timing of surge events is crucial in predicting extreme water levels and assessing flood hazard in estuaries with a large tidal range (Batstone et al. 2013).

Influence of the Storm Surge Shape

The shape of the storm surge component with time (surge skewness) influences variability in extreme water levels and total surge in the Severn Estuary model domain. As seen in Fig. 6, a storm surge with a positive skewness appears to create a greater range in maximum water elevation at every point along the deepest channel of the estuary. Positive skewness can act to extend the duration of high water, and therefore increase water volume and surge inflow in the estuary. This could help to amplify the tide further up the estuary (as shallow water effects are reduced) (Proudman 1955b). With distance up-estuary, the surge skewness may become more negative or more positive consistent with the magnitude of the local interaction growing with tide-surge propagation up-estuary. The shape and time profile of each storm surge generated on the continental shelf varies between historical extreme water level events, and skewness of the storm surge component could be just one of many characteristics controlling this driver of flood hazard. If shape of a storm surge can be forecast or detected early, then locations in the upper estuary can be warned of consequential amplification of the flood hazard.

Previous studies have highlighted the influence surge shape may have on water levels in the coastal zone (Proudman

1955b; McMillan et al. 2011a). The Environment Agency has provided time-integrated duration design surge shapes at tide gauge locations around the UK coastline, from the 15 largest ‘skew surge’ events on record (McMillan et al. 2011a). The skewness, i.e. the measure of asymmetry, of the design surge shapes for tide gauge locations in the Severn Estuary were calculated and shown to have a negative skewness over a 60-h window (Ilfracombe -0.46 , The Mumbles, -0.26). These results indicate that storm surges with a negative skewness create a constrained range of extreme water elevations in the Severn Estuary model domain. Therefore, it would be diligent to undertake sensitivity testing of surge skewness derived from historic events to understand variability in extreme water levels.

Estuarine Form as a Pathway to Increase Flood Hazard

The severity of the extreme water level event, timing and surge skewness each contribute to the source of a potential flood event. Pathways are the mechanisms that convey floodwaters from physical drivers, to impact receptors (people, businesses and the built environment). These are often considered to be overland flows, flows in river channels and sea defence overtopping (Narayan et al. 2012). However, it is known that estuaries and coastal inlets can affect surge and wave propagation in the coastal zone (HR Wallingford 2004). Therefore, the geometry, bathymetry and form of the estuary should be considered a pathway or source in itself, and influence on flood hazard acknowledge.

The geometry of the Severn Estuary has a strong control on tide-surge propagation and total surge contribution to water levels. The greatest percentage change in maximum total surge elevation in the model domain occurs when the peak of the surge occurs significantly before or after tidal high water, in locations further up-estuary, e.g. Portbury and Sharpness. As the peak of the surge occurs closer to low water, there may be greater effect bottom friction and shallow water effects on tidal dynamics (Proudman 1955b). Flood hazard is reduced when changes in maximum total surge elevation increase. Total surge, including a meteorological component and tide-surge interaction component, does not appear to contribute to extreme water levels, but appears to create variability in extreme water levels in the upper estuary.

The smallest change in maximum total surge elevation in the model domain can be seen when the peak of the surge occurs within 1 h of tidal high water. This is a phenomenon often observed along the west coast of Britain: if the peak of a storm surge occurs close to the time of tidal high water then there is very little time for interactions to develop and little effect of bottom friction due to the greater volumetric contribution of the tide and surge (Proctor and Flather 1989; Horsburgh and Wilson

2007; Jones and Davies 2007). Tide-surge interaction may not contribute to extreme water levels in the estuary but the shallow, narrow estuary creates variability which should be considered to potentially increase exposure and consequences of coastal towns in the upper estuary.

The geometry of the estuary has a particularly strong control over the location of maximum tidal range in the estuary, close to Portbury (Figs. 5 and 6). Maximum overall water elevation in the Severn Estuary model domain consistently occurs close to Portbury. This is known to be as a result of the funnelling and friction effect in the estuary (Dyer 1995). Tides and surges are amplified from the deeper part of the estuary, through the increasingly narrow, shallow channel towards Portbury (Pye and Blott 2010). This funnelling effect, due to channel convergence, increases tidal range to a maximum within the estuary at Portbury (Lennon 1963). The cyclic semi-diurnal tide is analogous to the incoming resonance from the west side of the Atlantic Ocean to the east (Gao and Adcock 2016), which further amplifies storm surges up-estuary (Liang et al. 2014). Beyond Portbury, frictional effects control the dampening of the tide as energy is lost and the tidal range decreases (Wolf 1981).

Further to this, human intervention in the estuary itself could influence how the physical drivers of flood hazard ('sources') move through the estuary. The location and design of sea defences, harbours and interventions (e.g. managed realignment schemes at Steart Marshes (Wright et al. 2011)) would also act to influence the magnitude and variability of extreme water levels (HR Wallingford 2003). These interventions would in turn also influence the damage caused and extent of coastal flooding that may be experienced as a result of the event. River discharge is another pathway to consider, and can induce interactions that lead to increases in the non-tidal residual elevation up to 0.35 m in the Severn Estuary (Maskell et al. 2014).

Flood hazard assessment, and application of the SPRC model at a local and regional scale, should consider that the form of a hyper-tidal estuary is a 'source' or 'pathway' in itself, influencing how floodwaters are conveyed through the system.

Implications for Local Management Needs in the Severn Estuary and Worldwide

When viewed in an operational context, these results help to identify contributions to the sources of flood hazard and identify the estuarine form as a source and pathway in itself which can act to exacerbate flood hazard. As seen in Fig. 7, the severity of an event appears to be the most important control on flood hazard in a hypertidal estuary. The events are stacked as a function of severity, and the 99th percentile event, 3rd January 2014, consistently produces the maximum water level

through the thalweg. The 'worst case' combination of variables to result in greatest flood hazard would be a 99th percentile event and concurrence of a storm surge peak with positive skewness and tidal high water. However, it should be considered that accurate bathymetry and boundary forcing data is important when testing hypothesis in estuaries (Pye and Blott 2014). The accuracy of models which aim to link estuarine hydrodynamic processes and form, e.g. extreme water levels is dependent on accurate bathymetry. The Severn Estuary model is forced at the tidal boundary with data from one tide gauge, which could limit how accurately water levels and interactions within the estuary are reproduced. There is a need for clear, accurate information to inform operational flood management, with the aim of reducing the hazard from flood events to the people who are located in flood-prone areas which should utilise the best available data (Pye and Blott 2010).

Freshwater flow can be an important control on tide-surge propagation in some hyper-tidal estuaries (Hoitink and Jay 2016). River discharge and its associated water levels can combine with storm surges driven by the same weather system (Svensson and Jones 2002), to alter the timing and magnitude of water levels within the estuary. Nonlinear interactions between extreme river discharge and storm surges can elevate residual water levels up to 0.35 m in idealised estuaries (Maskell et al. 2014), and have been shown to influence sub-tidal friction and the timing of high and low water in the River Mahakam, Indonesia (Sassi and Hoitink 2013). Heavy rainfall and spring meltwater, which result in high discharges have been shown to inhibit tide-surge propagation up-estuary in the LaHave Estuary, Nova Scotia (Webster et al. 2014); however, dredging activities in the Modaomen Estuary, China, facilitates inland propagation of surges and can alter salinisation within an estuary (Cai et al. 2012). Flood hazard and inundation extents are largely controlled by surge elevation, except in the most extreme river discharge events (Maskell et al. 2014). Freshwater flow and tide-surge propagation are not statistically independent (Svensson and Jones 2002), and their combined impact is controlled by the timing of peak river discharge, geometry of the estuary and floodplains and human intervention within the estuary.

Under changing climate and sea-level rise, the methods and results presented here could change due to changes in tidal range, which would alter tide-surge interaction (Robins et al. 2016). Deeper water will change frictional influence, and the tipping point between the effect of funnelling and friction effect is likely to change. This will have an impact on the location of maximum tidal range within the estuary and tidal asymmetry (Robins et al. 2014). In addition to this, rising sea level may alter channel depths or alter tidal prism (Passeri et al. 2015), therefore fundamentally altering the feedback

between estuarine form and water level. In some coastal regions, sea-level rise will increase the magnitude and frequency of extreme storm events, leading to increased flood hazard (Nicholls et al. 2011; Woodworth et al. 2009). Therefore, the need for accurate operational forecasting of extreme storm events will increase under changing climates.

Analysis of barotropic tide-surge propagation in a hyper-tidal estuary has shown sensitivity of coastal flood hazard, generated from the water level boundary conditions, to storm timing, storm surge shape and event severity. This knowledge is of significance to operational modelling for local predictions and flood hazard assessments. However, sources of coastal flood hazard are not just limited to the contributions of astronomical tide and storm surges to water level, but also wave run-up and overwashing or overtopping, driven by coincidental sea state (Prime et al. 2016). Locally-generated wind waves and propagating swell waves, generated by an offshore storm, which coincide with an extreme water level can increase flood hazard at the coast (Wolf 2009; Pye and Blott 2010). Maximum wave height at time of tidal high water can be significant for coastal flooding (Fairley et al. 2014), and runup associated with direct wind setup or breaking offshore waves can influence defence overtopping and breaching (Cheng et al. 2015). Future work to consider the influence of swell and wind waves on water levels and uncertainty in wave forcing has the potential to provide improved understanding of the combined effect of tide-surge-river-waves on water levels in a hypertidal estuary. Model outputs from a study into the combined effect of tide-surge-river-waves on water levels can be used to force an inundation model (Maskell et al. 2014; Prime et al. 2015), to simulate the area of maximum inundation from extreme water level events. Modelling studies that combine tide-surge-river-wave propagation with depth and extent of inundation can be effective for floodplain development, flood defences and protection for critical infrastructure in the estuary.

Conclusion

There is a need to understand the combination and variability of physical drivers contributing to flood hazard in hyper-tidal estuaries, due to their dynamic nature and increasing development pressures. Delft3D-FLOW is used to simulate tide-surge propagation in a hyper-tidal estuary to understand the mechanisms controlling extreme water levels, which contribute to flood hazard. Long-term tide gauge records are used to consider the influence of event severity, the timing of the peak of the surge relative to tidal high water and storm surge skewness on spatial variability of historic extreme water level events in the Severn Estuary

example. Event severity is the most important control on extreme water levels when modelling tide-surge propagation on a local scale. The shape of the storm surge component with time, classified using surge skewness as a measure of asymmetry, and timing of the storm surge peak relative to tidal high water influence spatial variability of water levels throughout the estuary. Demonstration of the shallow water effect shows the effect estuarine form can have on the variability of extreme water levels; therefore, it is crucial to have accurate bathymetry and boundary conditions to capture these changes throughout the estuary. However, maximum total surge elevation does not appear to significantly contribute to flood hazard as the maximum contribution occurs during the rise of an adjacent tide to that of the storm tide. The results can be interpreted in the context of the SPRC model, to identify the combined effect of factors which contribute to extreme water levels for local scale, flood hazard management. The methodology can be applied to understand past extreme water level events, and in turn help to identify future flood hazard in hypertidal estuaries worldwide.

Acknowledgements The authors thank colleagues at the British Oceanographic Data Centre (BODC) for providing tidal data; Magnox for providing tidal data; Environment Agency for providing tidal data and river gauge data; Gloucester Harbour Trustees for providing tidal data; and EDINA for bathymetric data. This work was supported by the Engineering and Physical Sciences Research Council as part of the Adaptation and Resilience of Coastal Energy Supply (ARCoES) project, grant number EP/I035390/1.

Open Access This article is distributed under the terms of the Creative Commons Attribution 4.0 International License (<http://creativecommons.org/licenses/by/4.0/>), which permits unrestricted use, distribution, and reproduction in any medium, provided you give appropriate credit to the original author(s) and the source, provide a link to the Creative Commons license, and indicate if changes were made.

References

- Archer, A.W. 2013. World's highest tides: hyper-tidal coastal systems in North America, South America and Europe. *Sedimentary Geology* 284–285: 1–25.
- As-Salek, J.A., and T. Yasuda. 2001. Tide–surge interaction in the Meghna estuary: most severe condition. *American Meteorological Society* 31: 3059–3072.
- Ballinger, R., and T. Stojanovic. 2010. Policy development and the estuary environment: a Severn estuary case study. *Marine Pollution Bulletin* 61 (1–3): 132–145.
- Batstone, C., M. Lawless, J. Tawn, K. Horsburgh, D. Blackman, A. McMillan, D. Worth, S. Laeger, and T. Hunt. 2013. A UK best-practice approach for extreme sea-level analysis along complex topographic coastlines. *Ocean Engineering* 71: 28–39.
- Brown, J.M., R. Bolaños, and A.J. Souza. 2014. Process contribution to the time-varying residual circulation in tidally dominated estuarine environments. *Estuaries and Coasts* 37 (5): 1041–1057.

- Cai, H., H.H.G. Savenije, Q. Yang, S. Ou, and Y. Lei. 2012. Influence of river discharge and dredging on tidal wave propagation: Modaomen estuary case. *Journal of Hydraulic Engineering* 138 (10): 885–896.
- Symonds, Capita. 2011. *Strategic flood risk assessment—level 2 Avonmouth / Severnside*. Bristol: Capita Symonds, Bristol City Council, South Gloucestershire Council, Lower Severn Drainage Board <https://www.southglos.gov.uk/documents/pte110072.pdf>.
- Chen, Y., W. Huang, and S. Xu. 2014. Frequency analysis of extreme water levels affected by sea-level rise in east and southeast coasts of China. *Journal of Coastal Research* 68: 105–112.
- Cheng, T.K., D.F. Hill, and W. Read. 2015. The contributions to storm tides in Pacific northwest estuaries: Tillamook Bay, Oregon, and the December 2007 storm. *Journal of Coastal Research* 31 (3): 723–734.
- Condon, A., and J. Veeramony. 2012. Development and validation of a coastal surge and inundation prediction system. *Oceans*: 1–8.
- Cornett, A., J. Cousineau, and I. Nistor. 2013. Assessment of hydrodynamic impacts from tidal power lagoons in the bay of Fundy. *International Journal of Marine Energy* 1: 33–54.
- Davies, J. 1964. A morphogenetic approach to world shorelines. *Zeitschrift für Geomorphologie* 8: 27–42.
- Desplanque, C., and D.J. Mossman. 2004. Tides and their seminal impact on the geology, geography, history, and socio-economics of the bay of Fundy, eastern Canada. *Atlantic Geology* 40 (1): 1–130.
- Desplanque, C., and D.J. Mossman. 1999. Storm tides of the Fundy. *American Geographical Society* 89 (1): 23–33.
- de Vries, H., A. Voorrips, M. Breton, J.C. Salomon, T. de Mulder, J. Ozer, K. Ruddick, Y. Krestenitis, and R. Proctor. 1995. A comparison of 2D storm surge models applied to three shallow European seas. *Environmental Software* 10 (1): 23–42.
- Dyer, K.R. 1995. Sediment transport processes in estuaries, in geomorphology and sedimentology of estuaries. *Developments in Sedimentology*: 423–449.
- Elliott, M., N.D. Cutts, and A. Trono. 2014. A typology of marine and estuarine hazards and risks as vectors of change: a review for vulnerable coasts and their management. *Ocean and Coastal Management* 93: 88–99.
- Fairley, L., R. Ahmadian, R.A. Falconer, M.R. Willis, and L. Masters. 2014. The effects of a Severn barrage on wave conditions in the Bristol Channel. *Renewable Energy* 68: 428–442.
- Familkhali, R., and S.A. Talke. 2016. The effect of channel deepening on tides and storm surge: a case study of Wilmington, NC. *Geophysical Research Letters* 43 (17): 9138–9147.
- Gao, C. and Adcock, T. A. A. 2016. Numerical investigation of resonance in the Bristol Channel. In: *Proceedings of the International Offshore and Polar Engineering Conference*. Rhodes, Greece, 26 June – 2 July 2016. International Society of Offshore and Polar Engineers.
- Gouldby, B. and Samuels, P. (2005) Language of risk. Report: T32-04-01. Wallingford: FLOODSite. http://www.floodsite.net/html/partner_area/project_docs/floodsite_language_of_risk_v4_0_p1.pdf.
- Grotiot, N., E.J. Anthony, a. Gardel, C. Gaucherel, C. Proisy, and J.T. Wells. 2008. Significant contribution of the 18.6 year tidal cycle to regional coastal changes. *Nature Geoscience* 1 (3): 169–172.
- Greenberg, D.A., W. Blanchard, B. Smith, and E. Barrow. 2012. Climate change, mean sea level and high tides in the bay of Fundy. *Atmosphere-Ocean* 50 (3): 261–276.
- Gronweld, R.A., and G. Meeden. 1984. Measuring skewness and kurtosis. *Journal of the Royal Statistical Society. Series D (The Statistician)* 33 (4): 391–399.
- Haigh, I.D., M.P. Wadey, T. Wahl, O. Ozsoy, R.J. Nicholls, J.M. Brown, K. Horsburgh, and B. Gouldby. 2016. Analysis: spatial and temporal analysis of extreme sea level and storm surge events around the coastline of the UK. *Scientific Data* 3: 1–14.
- Heaps, N.S. 1983. Storm surges, 1967–1982. *Geophysical Journal of the Royal Astronomical Society* 74 (1): 331–376.
- Hoitink, A.J.F., and D.A. Jay. 2016. Tidal river dynamics: implications for deltas. *Reviews of Geophysics* 54 (1): 240–272.
- Horrillo-Caraballo, J.M., D.E. Reeve, D. Simmonds, S. Pan, A. Fox, R. Thompson, S. Hoggarth, S.S.H. Kwan, and D. Greaves. 2013. Application of a source-pathway-receptor-consequence (S-P-R-C) methodology to the Teign estuary, UK. *Journal of Coastal Research: Special Issue - International Coastal Symposium* 65 (2): 1939–1944.
- Horsburgh, K., and M. Horritt. 2006. The Bristol Channel floods of 1607—reconstruction and analysis. *Weather* 61 (10): 272–277.
- Horsburgh, K.J., and C. Wilson. 2007. Tide-surge interaction and its role in the distribution of surge residuals in the North Sea. *Journal of Geophysical Research: Oceans* 112 (8): 1–13.
- Wallingford, H.R. 2003. *Risk, performance and uncertainty in flood and coastal defence—a review, SR 587*. 2nd ed. UK: Wallingford http://sciencesearch.defra.gov.uk/Document.aspx?Document=FD2302_3433_TRP.pdf.
- Wallingford, H.R. 2004. *Best practice in coastal flood forecasting R&D technical report FD2206/TR1*. UK: Wallingford http://evidence.environment-agency.gov.uk/FCERM/Libraries/FCERM_Project_Documents/FD2206_3912_TRP_pdf.sflb.ashx.
- Irish, J.L., and R. Cañizares. 2009. Storm-wave flow through tidal inlets and its influence on bay flooding. *Journal of Waterway, Port, Coastal, and Ocean Engineering* 135 (April): 52–60.
- Jones, J.E., and A.M. Davies. 2007. Influence of non-linear effects upon surge elevations along the west coast of Britain. *Ocean Dynamics* 57 (4–5): 401–416.
- Jones, O.P., O.S. Petersen, and H. Kofoed-Hansen. 2007. Modelling of complex coastal environments: Some considerations for best practice. *Coastal Engineering* 54 (10): 717–733.
- Kron, W. 2009. Flood risk = hazard · values · vulnerability. *Water International* 30 (1): 58–68.
- Lennon, G. 1963. The identification of weather conditions associated with the generation of major storm surges along the west coast of the British Isles. *Quarterly Journal of the Royal Meteorological Society* 89: 381–394.
- Leonardi, N., A.S. Kolker, and S. Fagherazzi. 2015. Interplay between river discharge and tides in a delta distributary. *Advances in Water Resources* 80: 69–78.
- Lesser, G.R., J.A. Roelvink, J.A.T.M. van Kester, and G.S. Stelling. 2004. Development and validation of a three-dimensional morphological model. *Coastal Engineering* 51 (8–9): 883–915.
- Lewis, M., G. Schumann, P. Bates, and K. Horsburgh. 2013. Understanding the variability of an extreme storm tide along a coastline. *Estuarine, Coastal and Shelf Science* 123: 19–25.
- Liang, D., J. Xia, R.A. Falconer, and J. Zhang. 2014. Study on tidal resonance in Severn estuary and Bristol Channel. *Coastal Engineering Journal* 56 (1): 1450002.
- Marvin, J.T., and A.T. Wilson. 2016. One dimensional, two dimensional and three dimensional hydrodynamic modeling of a Dyked Coastal River in the bay of Fundy. *Journal of Water Management Modeling* 25 (C404): 1–13.
- Maskell, J., K. Horsburgh, M. Lewis, and P. Bates. 2014. Investigating river-surge interaction in idealised estuaries. *Journal of Coastal Research* 30 (2): 248–259.
- McGranahan, G., D. Balk, and B. Anderson. 2007. The rising tide: assessing the risks of climate change and human settlements in low elevation coastal zones. *Environment and Urbanization* 19 (1): 17–37.
- McMillan, A., D. Worth, and D.M. Lawless. 2011a. *Coastal flood boundary conditions for UK mainland and islands. Project SC060064 TR4. Practical guidance design sea levels*. Peterborough: Environment Agency https://www.gov.uk/government/uploads/system/uploads/attachment_data/file/291222/scho0111btck-e-e.pdf.

- McMillan, A., C. Baststone, D. Worth, J. Tawn, K. Horsburgh, and M. Lawless. 2011b. *Coastal flood boundary conditions for UK mainland and islands project: SC060064/TR2: design sea levels*. Peterborough: Environment Agency https://www.gov.uk/government/uploads/system/uploads/attachment_data/file/291216/scho0111btki-e-e.pdf.
- Menéndez, M. and Woodworth, P. 2010. Changes in extreme high water levels based on a quasi-global tide-gauge data set. *Journal of Geophysical Research: Oceans* 115(C10): 1:15.
- Monbalieu, J., Z. Chen, D. Felts, J. Ge, F. Hissel, J. Kappenberg, S. Narayan, R.J. Nicholls, N. Ohle, D. Schuster, J. Sothmann, and P. Willems. 2014. Risk assessment of estuaries under climate change: Lessons from Western Europe. *Coastal Engineering* 87: 32–49.
- Narayan, S., S. Hanson, R.J. Nicholls, D. Clarke, P. Willems, V. Ntegeka, and J. Monbalieu. 2012. A holistic model for coastal flooding using system diagrams and the source-pathway-receptor (SPR) concept. *Natural Hazards and Earth System Sciences* 12 (5): 1431–1439.
- Nicholls, R.J., N. Marinova, J.A. Lowe, S. Brown, P. Vellinga, D. de Gusmão, and J. Hinkel. 2011. Sea-level rise and its possible impacts given a 'beyond 4 degrees C world' in the twenty-first century. *Philosophical transactions of the Royal Society A: mathematical, physical and engineering sciences* 369 (1934): 161–181.
- Oosterwind, D., A. Rau, and A. Zaiko. 2016. Drivers and pressures—untangling the terms commonly used in marine science and policy. *Journal of Environmental Management* 181: 8–15.
- Pan, C.-H., B.-Y. Lin, and X.-Z. Mao. 2007. Case study: Numerical modeling of the tidal bore on the Qiantang River, China. *Journal of Hydraulic Engineering* 133 (2): 130–138.
- Passeri, D.L., S.C. Hagen, S.C. Medeiros, M.V. Bliskie, K. Alizad, and D. Wang. 2015. The dynamic effects of sea level rise on low-gradient coastal landscapes: a review. *Earth's Future* 3 (6): 159–181.
- Pender, G., and S. Néelz. 2007. Use of computer models of flood inundation to facilitate communication in flood risk management. *Environmental Hazards* 7 (2): 106–114.
- Pottier, N., E. Penning-Roswell, S. Tunstall, and G. Hubbert. 2005. Land use and flood protection: contrasting approaches and outcomes in France and in England and Wales. *Applied Geomorphology* 25 (1): 1–27.
- Prime, T., J.M. Brown, and A.J. Plater. 2015. Physical and economic impacts of sea-level rise and low probability flooding events on coastal communities. *PLoS One* 10 (2): 1–28.
- Prime, T., J.M. Brown, and A.J. Plater. 2016. Flood inundation uncertainty: the case of a 0.5% annual probability flood event. *Environmental Science & Policy* 56: 1–9.
- Proctor, R., and R.A. Flather. 1989. Storm surge prediction in the Bristol Channel—the floods of 13 December 1981. *Continental Shelf Research* 9 (10): 889–918.
- Proudman, J. 1955a. The effect of friction on a progressive wave of tide and surge in an estuary. *Proceedings of the Royal Society of London. Series A, Mathematical and Physical Sciences* 233 (1194): 407–418.
- Proudman, J. 1955b. The propagation of tide and surge in an estuary. *Proceedings of the Royal Society of London, Series A, Mathematical and Physical Sciences* 231 (1184): 8–24.
- Pye, K., and S.J. Blott. 2010. A consideration of “extreme events” at Hinkley point, technical report series 2010, no. In *109 Ed 2*. Berkshire: Kenneth Pye Associates Ltd. <https://infrastructure.planninginspectorate.gov.uk/wp-content/ipc/uploads/projects/EN010001/EN010001-005181-HPC-NNBPEA-XX-000-RET-000182%201.pdf>.
- Pye, K., and S.J. Blott. 2014. The geomorphology of UK estuaries: the role of geological controls, antecedent conditions and human activities. *Estuarine, Coastal and Shelf Science* 150: 196–214.
- Quinn, N., M. Lewis, M.P. Wadey, and I.D. Haigh. 2014. Assessing the temporal variability in extreme storm-tide time series for coastal flood risk assessment. *Journal of Geophysical Research: Oceans* 119: 2227–2237.
- Reynolds, C.S. and West, J.R. 1988. Stratification in the Severn Estuary—Physical aspects and biological consequences. Ambleside: Freshwater Biological Association. http://www.environmentdata.org/archive/fbalc:62/OBJ/x34_ReynoldsC.S.J.R.West1988.pdf.
- Robins, P.E., M.J. Lewis, J.H. Simpson, E.R. Howlett, and S.K. Malham. 2014. Future variability of solute transport in a macrotidal estuary. *Estuarine, Coastal and Shelf Science* 151: 88–99.
- Robins, P.E., M.W. Skow, M.J. Lewis, L. Gimenez, A.G. Davis, S.K. Malham, S.P. Neill, J.E. McDonald, T.A. Whitton, S.E. Jackson, and C.F. Jago. 2016. Mpaact of climate change on UK estuaries: a review of past trends and potential projections. *Estuarine, Coastal and Shelf Science* 169: 119–135.
- Sassi, M.G., and A.J.F. Hoitink. 2013. River flow controls on tides and tide-mean water level profiles in a tidal freshwater river. *Journal of Geophysical Research Letters* 118: 4139–4151.
- Sayers, P.B., J.W. Hall, and I.C. Meadowcroft. 2002. Towards risk-based flood hazard management in the UK. *Civil Engineering* 150: 36–42.
- SeaZone Solutions Ltd. 2013. Gridded bathymetry: 1 Arcsecond [ascii], Scale 1:50,000, Tile: NW 55050025, NW 55050030, NW 55050035, NW 55050040, NW 55050045, NW 55100030, NW 55100035, NW 55100040, NW 55100045, NW 55150025, NW 55150030, NW 55150035, NW 55150040, NW 55150045, Updated August 2013, Crown Copyright / SeaZone Solutions Ltd., UK. Using: EDINA Marine Digimap Service, <http://edina.ac.uk/digimap>, Downloaded January 2016.
- Shanze, J. 2006. Flood risk management—a basic framework. In *Flood risk management: hazards, vulnerability and mitigation measures*, ed. J. Shanze, E. Zeman, and J. Marsalek, 1–20. The Netherlands: Springer.
- Sinha, P.C., I. Jain, N. Bhardwaj, A.D. Rao, and S.K. Dube. 2008. Numerical modeling of tide-surge interaction along Orissa coast of India. *Natural Hazards* 43: 413–427.
- Smith, R.A.E., P.D. Bates, and C. Hayes. 2012. Evaluation of a coastal flood inundation model using hard and soft data. *Environmental Modelling and Software* 30: 35–46.
- Spencer, T., S.M. Brooks, B.R. Evans, J.A. Tempest, and I. Moller. 2015. Southern North Sea storm surge event of 5 December 2013: water levels, waves and coastal impacts. *Earth-Science Reviews* 146: 120–145.
- Svensson, C., and D.A. Jones. 2002. Dependence between extreme sea surge, river flow and precipitation in eastern Britain. *International Journal of Climatology* 22 (10): 1149–1168.
- Uncles, R.J. 1981. A numerical simulation of the vertical and horizontal M2 tide in the Bristol Channel and comparisons with observed data. *Limnology and Oceanography* 26 (3): 571–577.
- Uncles, R.J. 2010. Physical properties and processes in the Bristol Channel and Severn estuary. *Marine Pollution Bulletin* 61 (1–3): 5–20.
- Wang, J., W. Gao, S. Xu, and L. Yu. 2012a. Evaluation of the combined risk of sea level rise, land subsidence, and storm surges on the coastal areas of Shanghai, China. *Climate Change* 115 (3–4): 537–558.
- Wang, L., X. Zhao, and Y. Shen. 2012b. Coupling hydrodynamic models with GIS for storm surge simulation: application to the Yangtze estuary and the Hangzhou Bay, China. *Frontiers in Earth Science* 6 (3): 261–275.
- Webster, T., K. McGuigan, K. Collins, and C. MacDonald. 2014. Integrated river and coastal hydrodynamic flood risk mapping of the LaHave River estuary and town of Bridgewater, Nova Scotia, Canada. *Water* 6 (3): 517–546.
- Williams, J., Wilson, C., Horsburgh, K. 2012. Re-analysis of the December 1981 storm surge event in the Bristol Channel using the current operational tide-surge model suite. National Oceanography Centre Research & Consultancy Report no. 26. National Oceanography Centre: Liverpool. http://nora.nerc.ac.uk/20129/1/NOC_R%26C_26.pdf

- Williams, J.A., and K.J. Horsburgh. 2013. Evaluation and comparison of the operational Bristol Channel model storm surge suite. In *National Oceanography Centre Research and consultancy report, 38*. Southampton: National Oceanography Centre http://nora.nerc.ac.uk/502138/1/NOC_R%26C_38.pdf.
- Williams, J., K. Horsburgh, J.A. Williams, and R.N.F. Proctor. 2016. Tide and skew surge independence: new insights for flood risk. *Geophysical Research Letters* 43 (12): 6410–6417.
- Willmott, C.J. 1981. On the validation of models. *Physical Geography* 2 (2): 184–194.
- Willmott, C.J., S.M. Robeson, and K. Matsuura. 2012. A refined index of model performance. *International Journal of Climatology* 32 (13): 2088–2094.
- Wolf, J. 1981. Surge-tide interaction in the North Sea and River Thames. In *Floods Due to High Winds and Tides*, ed. D.H. Peregrine, 75–94. Elsevier, New York.
- Wolf, J. 2009. Coastal flooding: impacts of coupled wave-surge-tide models. *Natural Hazards* 49 (2): 241–260.
- Woodworth, P.L., F.N. Teferle, R.M. Bingley, I. Shennan, and S.D. Williams. 2009. Trends in UK mean sea level revisited. *Geophysical Journal International* 176 (1): 19–30.0.
- Woth, K., R. Weisse, and H. von Storch. 2006. Climate change and North Sea storm surge extremes: an ensemble study of storm surge extremes expected in a changed climate projected by four different regional climate models. *Ocean Dynamics* 56 (1): 3–15.
- Wright, A., Shipton, J., Carroll, B., Armstrong, S. 2011. Lessons for designing managed realignment sites along hyper tidal estuaries—a case study on the Bristol port company's Steart habitat creation scheme. In: *Proceedings of the ICE Coastal Management 2011 Conference*. Belfast, UK, 15–16 November 2011.
- Xia, J., Falconer, R., Lin, B. 2010. Impact of different tidal renewable energy projects on the hydrodynamic processes in the Severn Estuary, UK. *Ocean Modelling*, 32 (1–2): 86–104.
- Zhang, J., Zhang, C., Wu, X. and Guo, Y. 2012. Astronomical tide and typhoon-induced storm surge in Hangzhou Bay, China. In: *Hydrodynamics - Natural Water Bodies* eds Schulz, H. E., Simoes, A. L. a., and Lobosco, R. J. InTech.